Electronic Supplementary Material (ESI) for New Journal of Chemistry.

Supplementary Information

Tetrathiafulvalene and π-extended tetrathiafulvalene pillar[5]arene conjugates: synthesis, electrochemistry and host-guest properties

Maksym Dekhtiarenko,[a,b] Gabriel Mengheres,[a] Eric Levillain,[a] Zoia Voitenko,[b] Iwona Nierengarten,[c] Jean-François Nierengarten,*[c] Sébastien Goeb*[a] and Marc Sallé*[a]

Table of Contents

SYNTHESIS

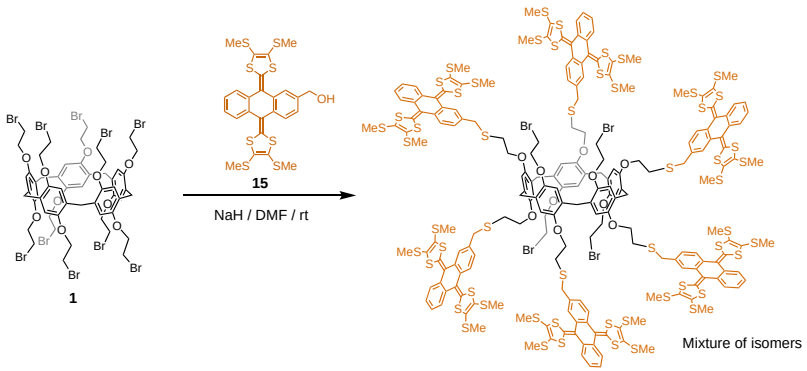

Scheme S1. Reaction of pillar[5]arene **1** with exTTF derivative **15** that did not lead to more than six substitutions.

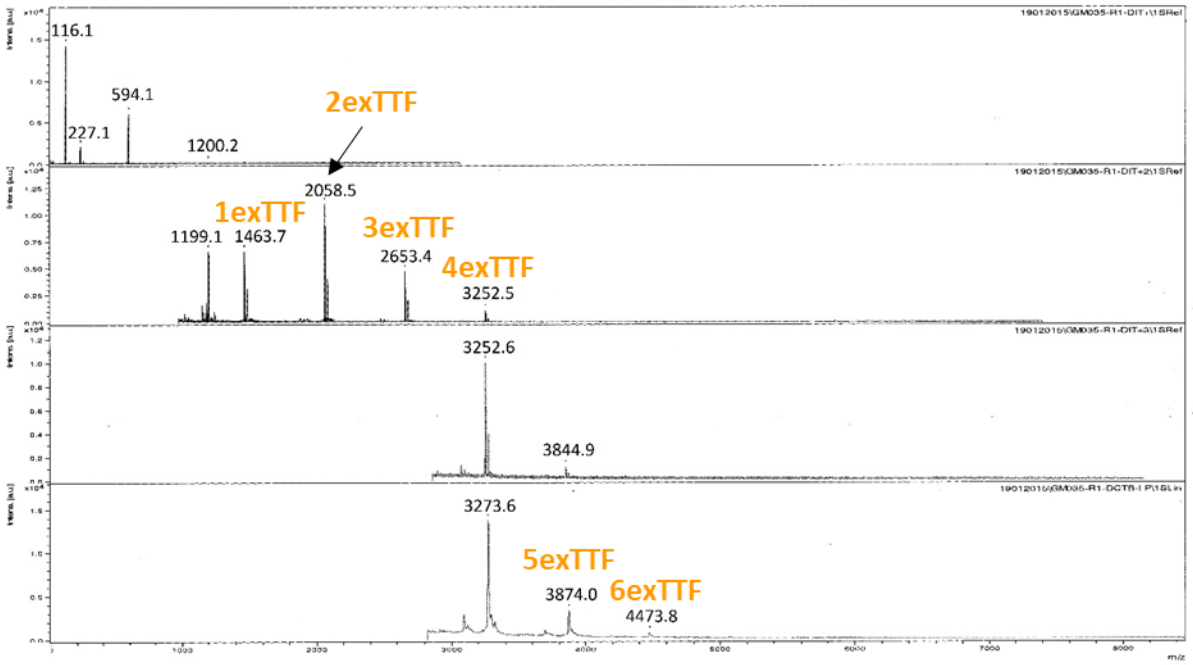

Figure S1. Mass spectrum corresponding to the synthesis depicted in scheme S1.

NMR, IR, UV-Vis and mass spectra

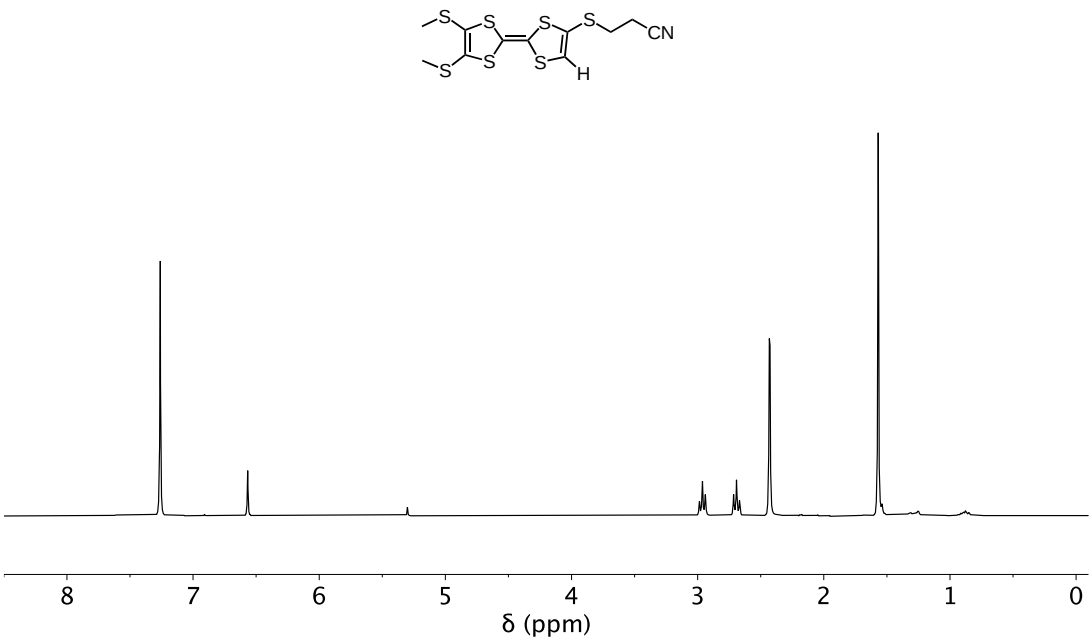

Figure S2. ^{1}H NMR spectrum of compound **2a** (300 MHz, $CDCl_3$, 298K).

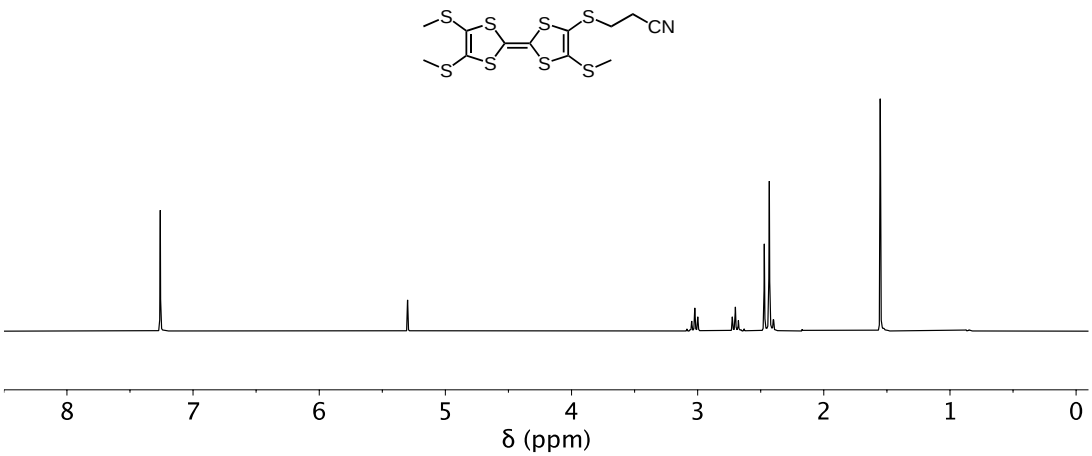

Figure S3. ^{1}H NMR spectrum of compound **2b** (300 MHz, $CDCl_3$, 298K).

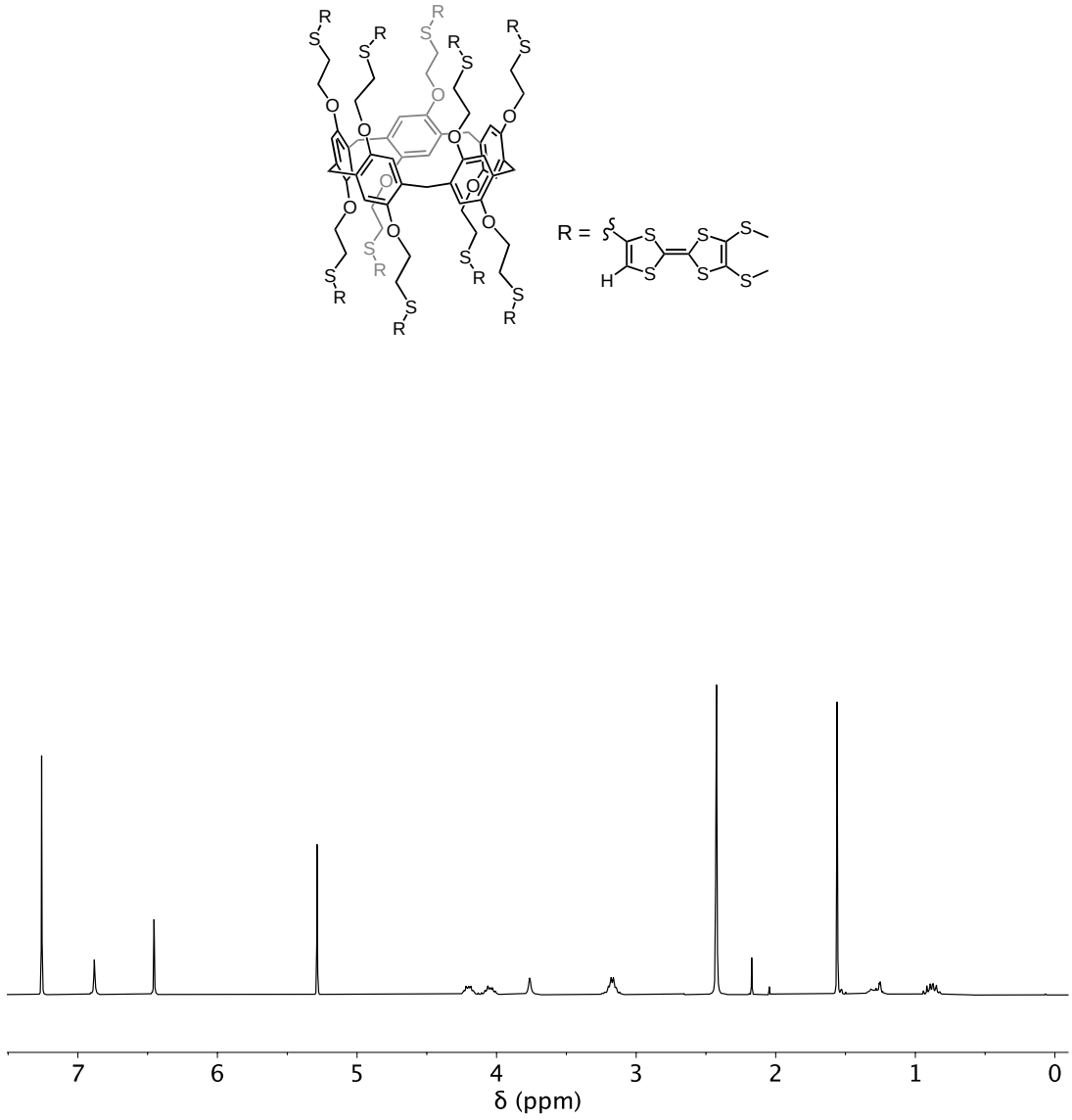

Figure S4a. ^{1}H NMR spectrum of compound **3a** (300 MHz, $CDCl_3$, 298K).

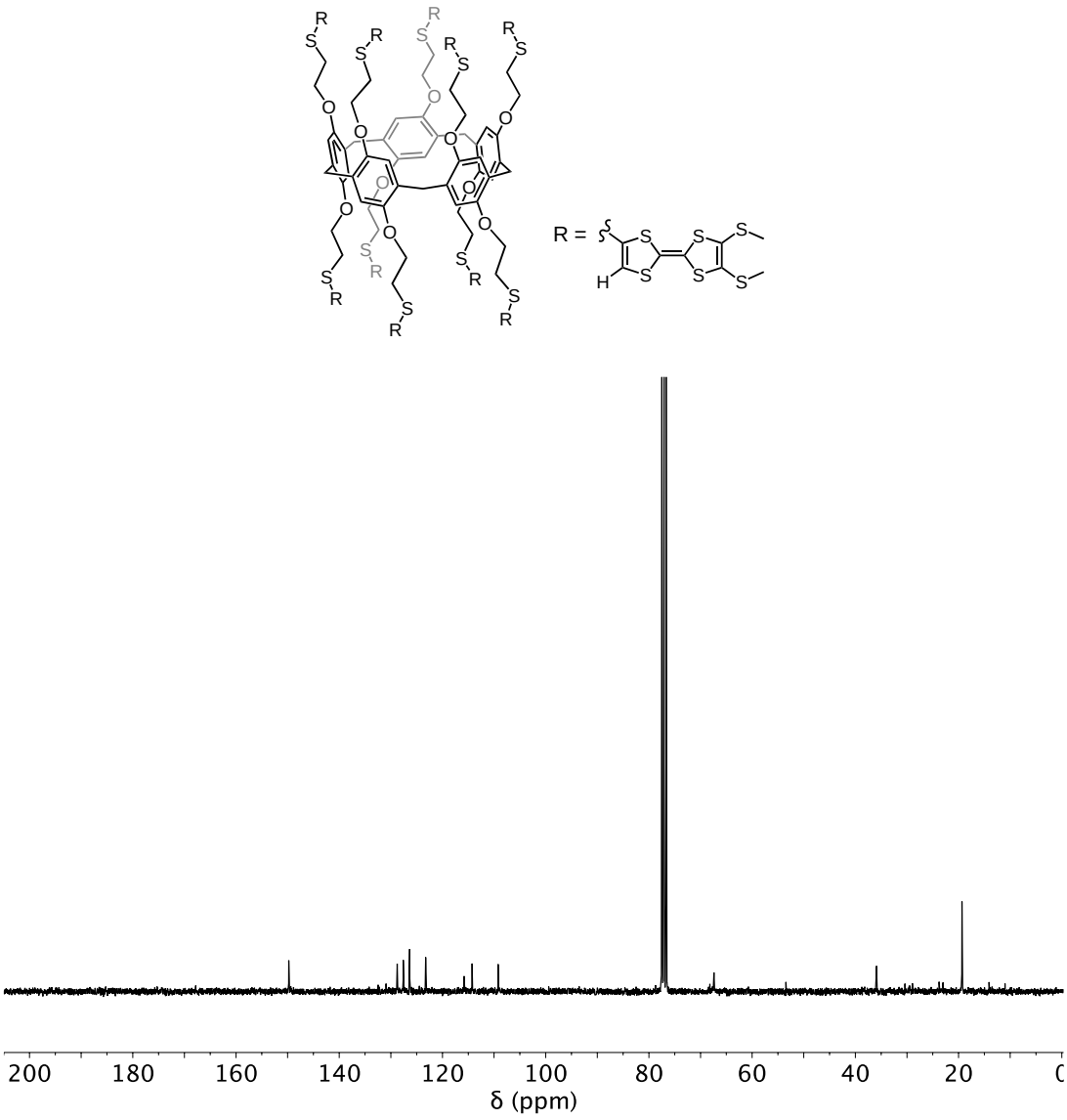

Figure S4b. ^{13}C NMR spectrum of compound **3a** (75 MHz, $CDCl_3$, 298K).

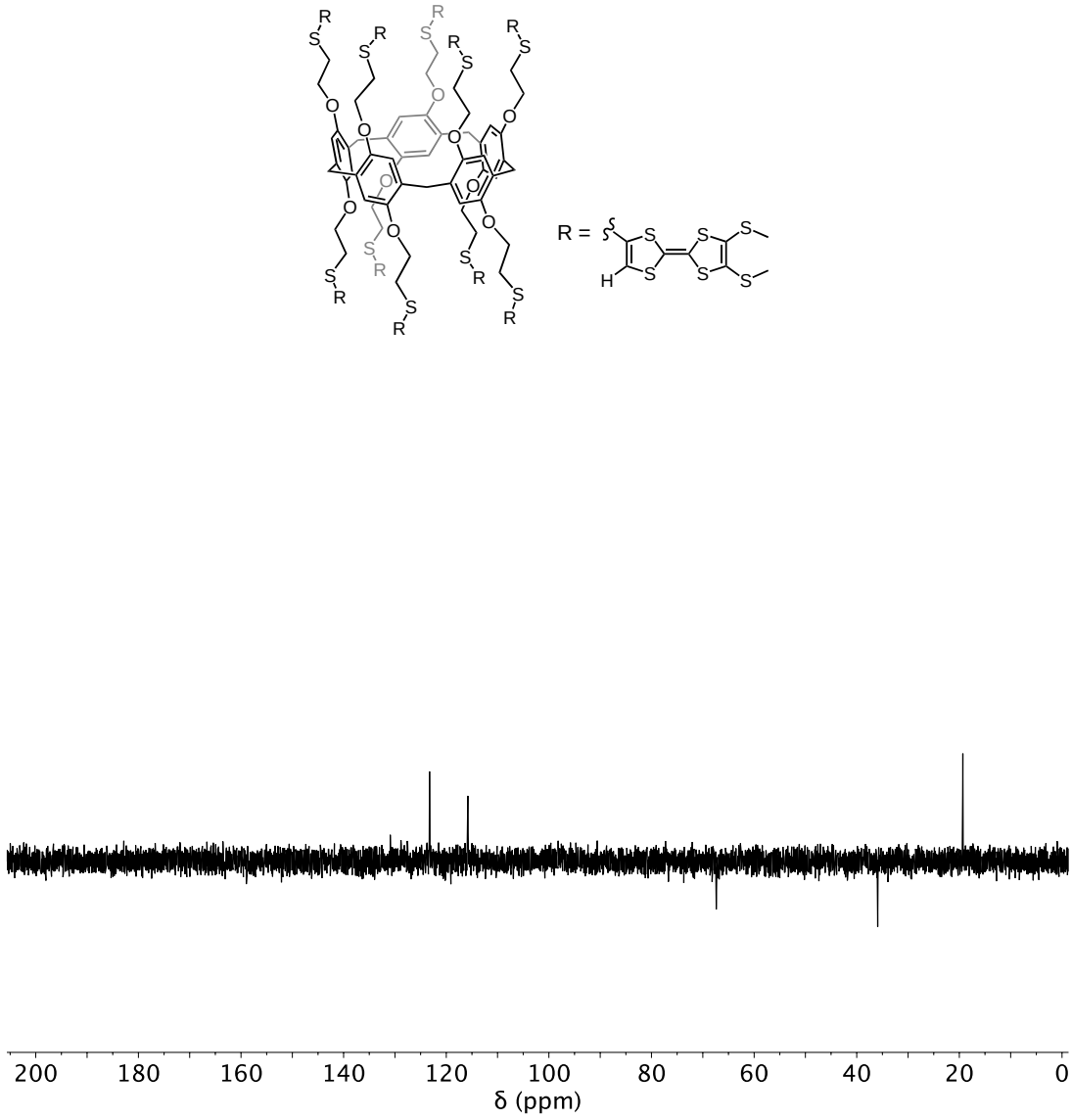

Figure S4c. DEPT spectrum of compound **3a** (75 MHz, $CDCl_3$, 298K).

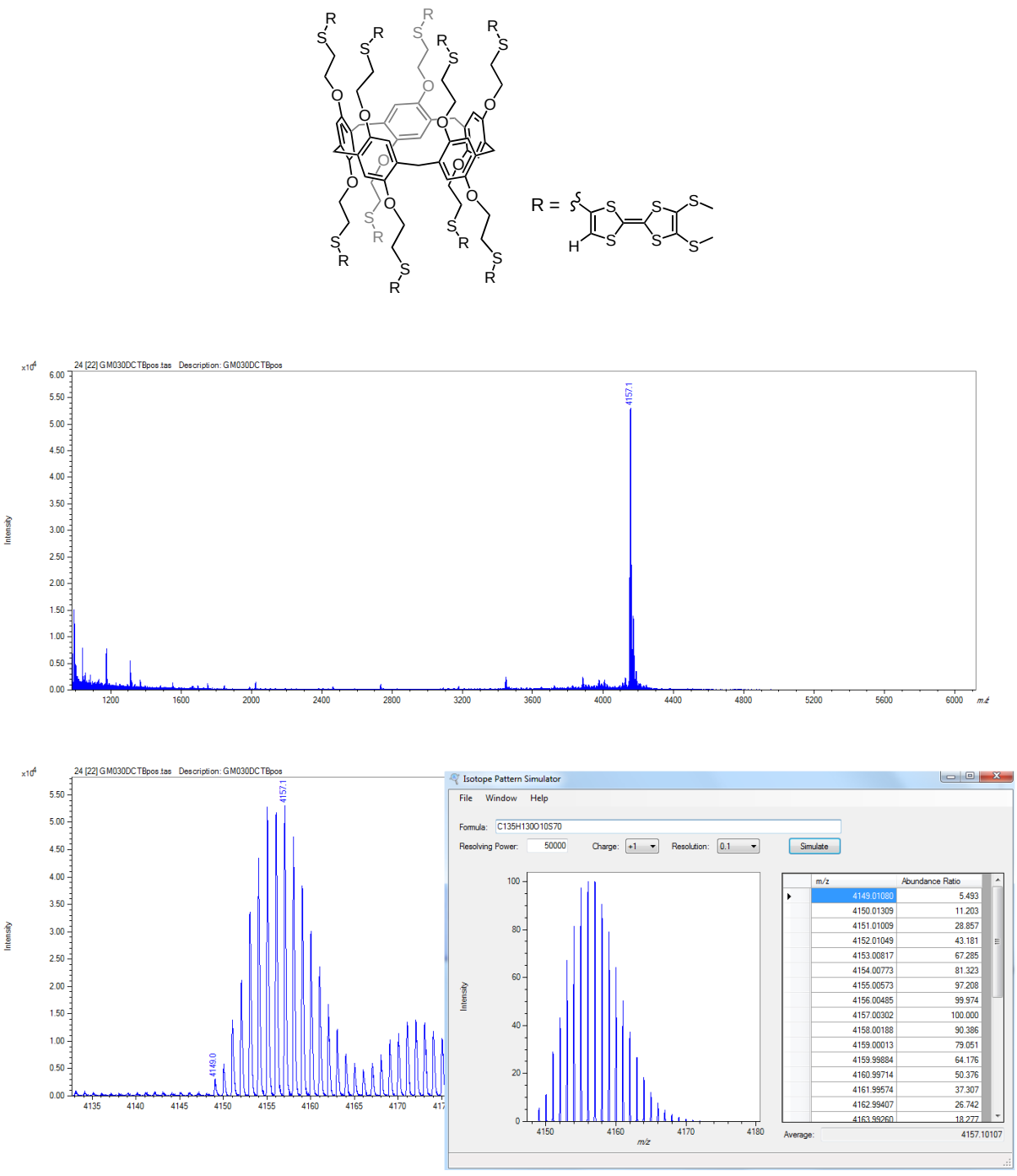

Figure S4d. MALDI-TOF mass spectrum of compound **3a**.

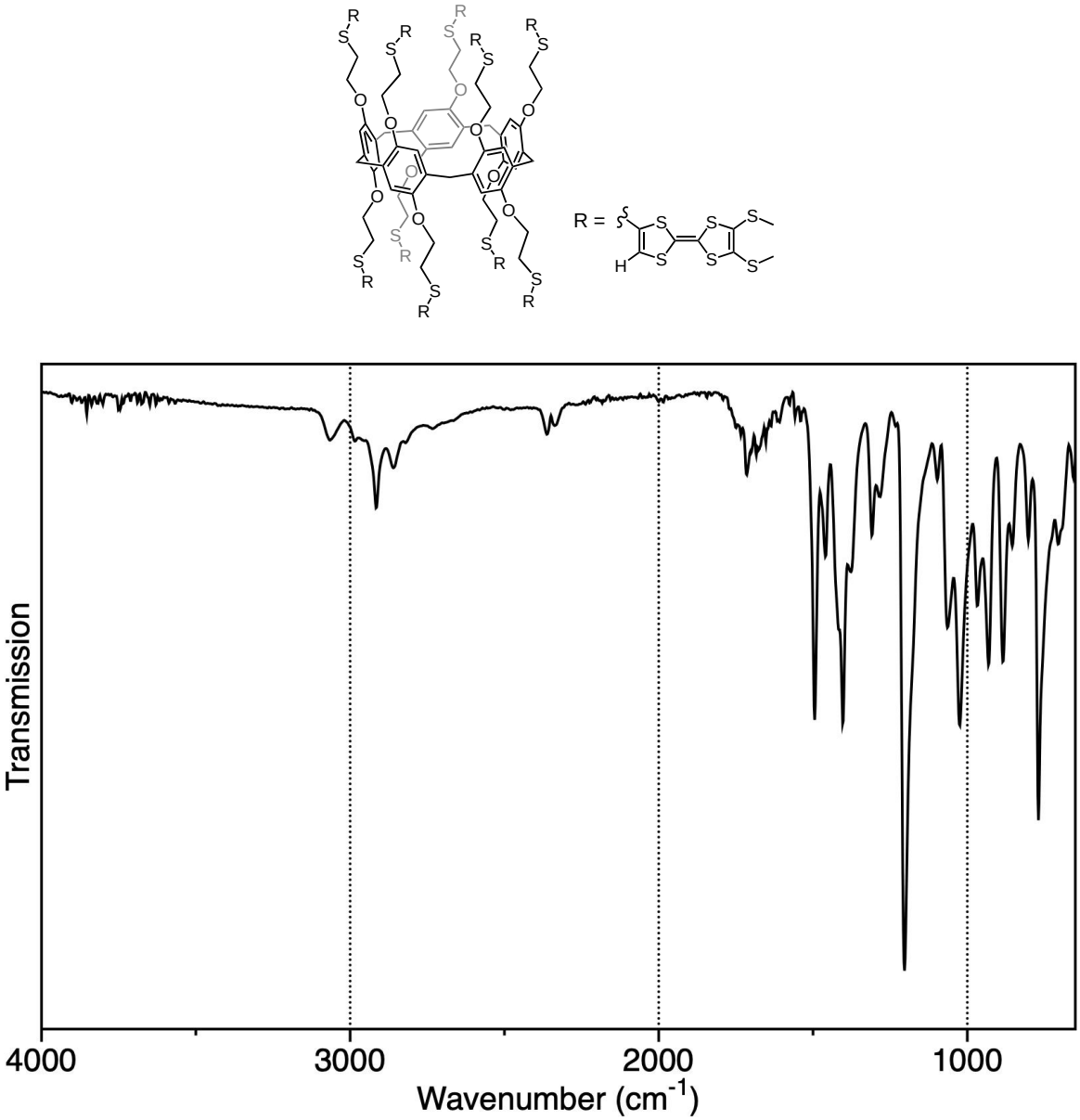

Figure S4e. IR spectrum of compound **3a**.

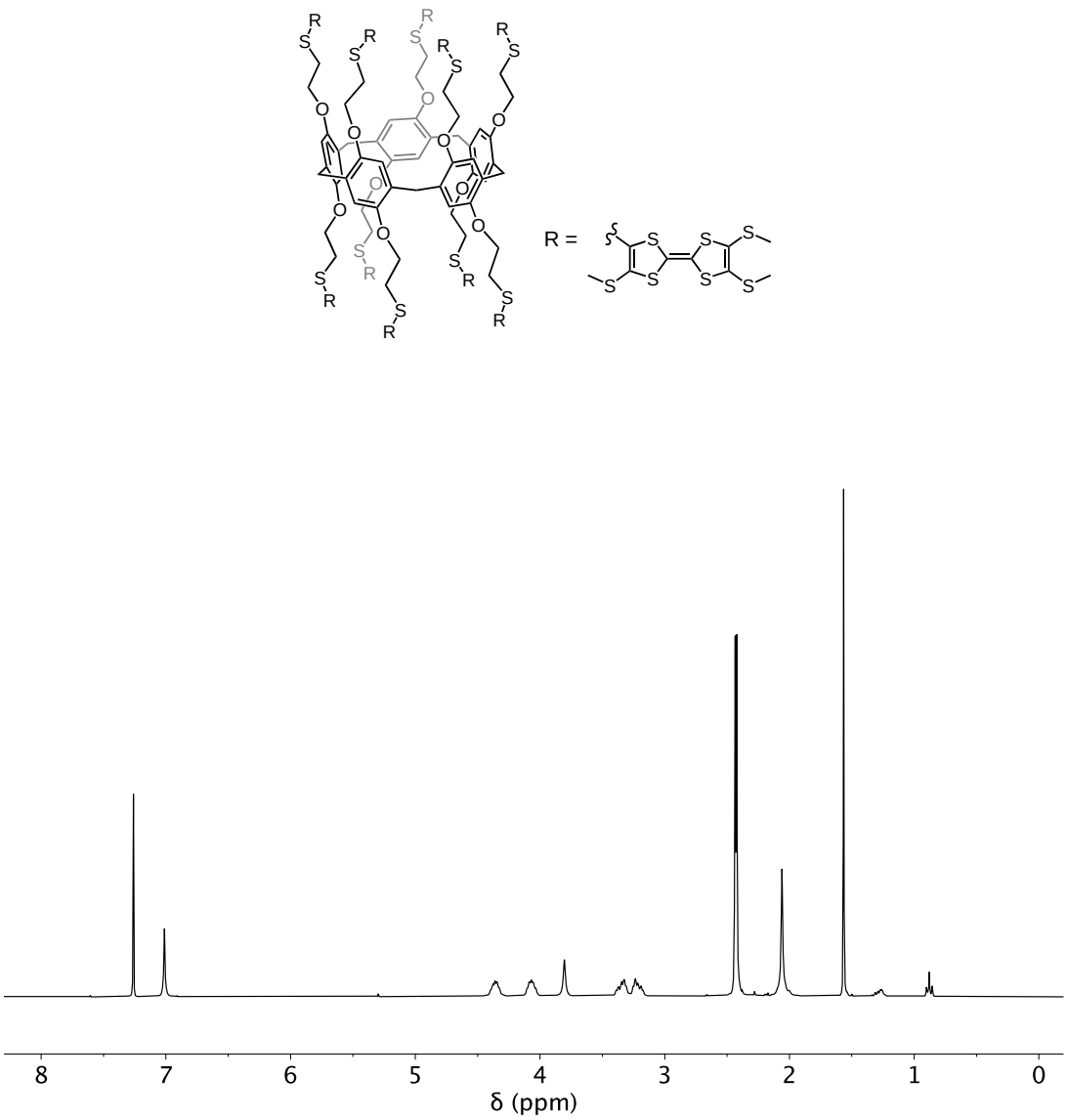

Figure S5a. ^{1}H NMR spectrum of compound **3b** (300 MHz, $CDCl_3$, 298K).

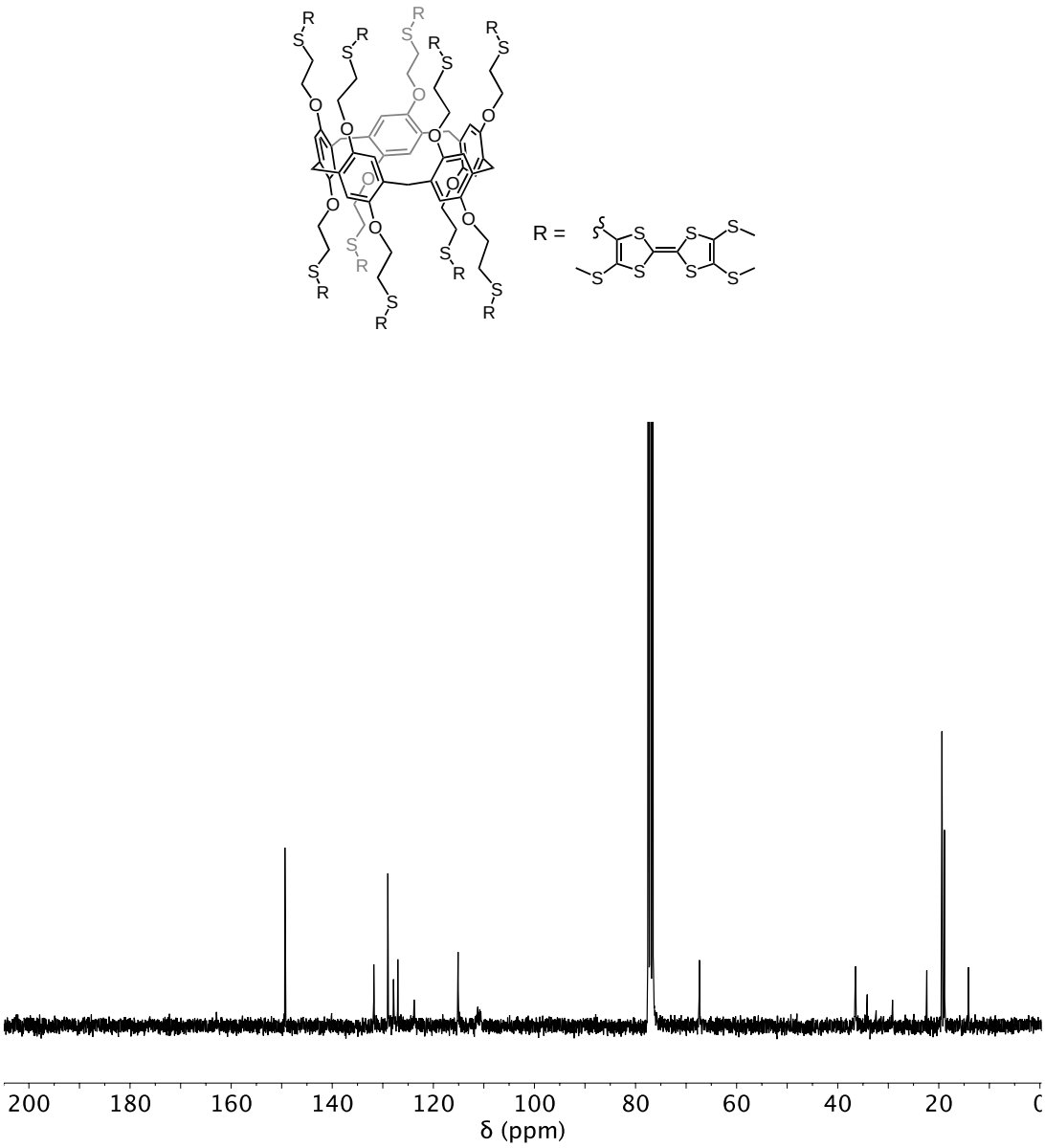

Figure S5b. ^{13}C NMR spectrum of compound **3b** (75 MHz, $CDCl_3$, 298K).

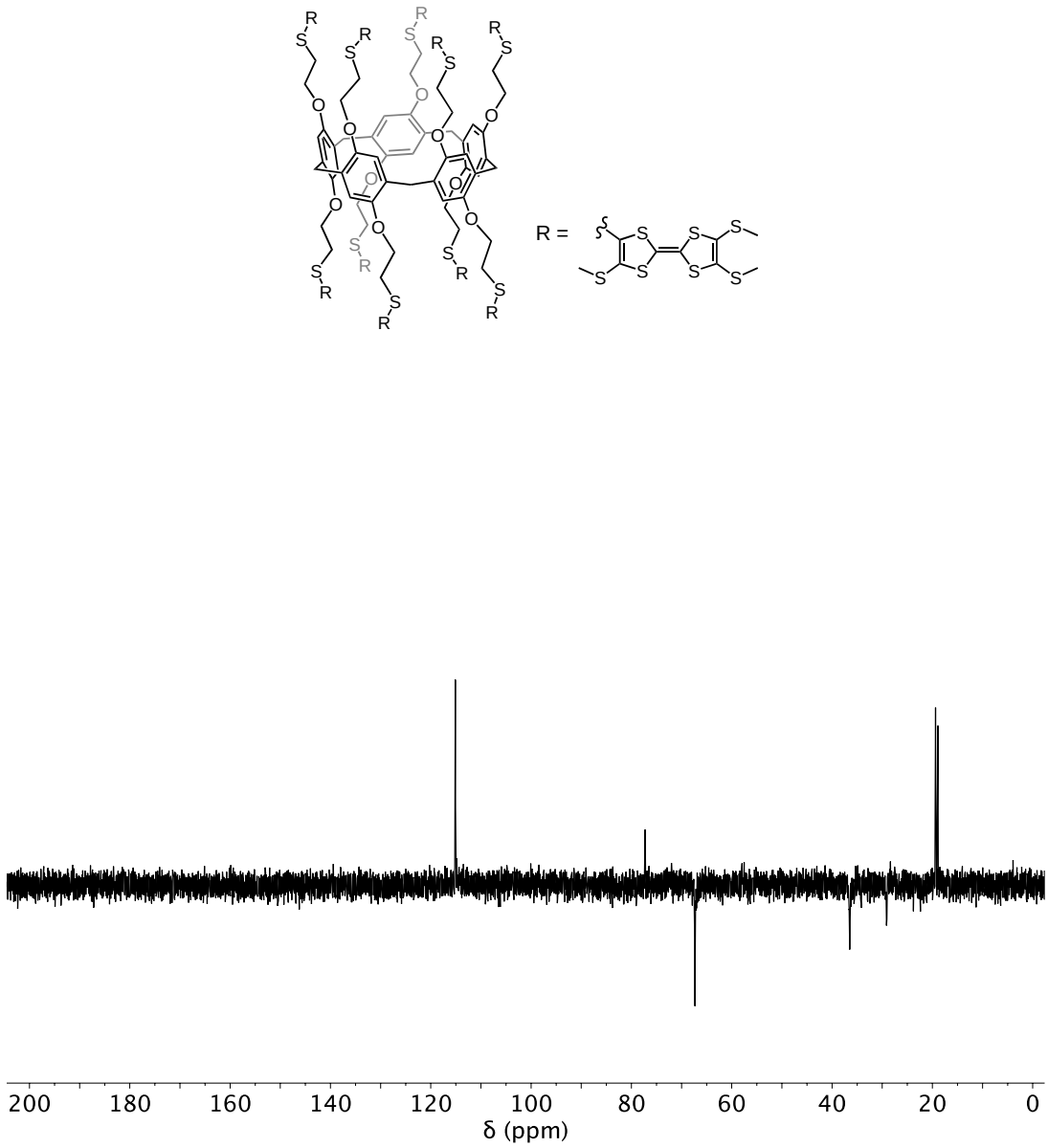

Figure S5c. DEPT spectrum of compound **3b** (75 MHz, $CDCl_3$, 298K).

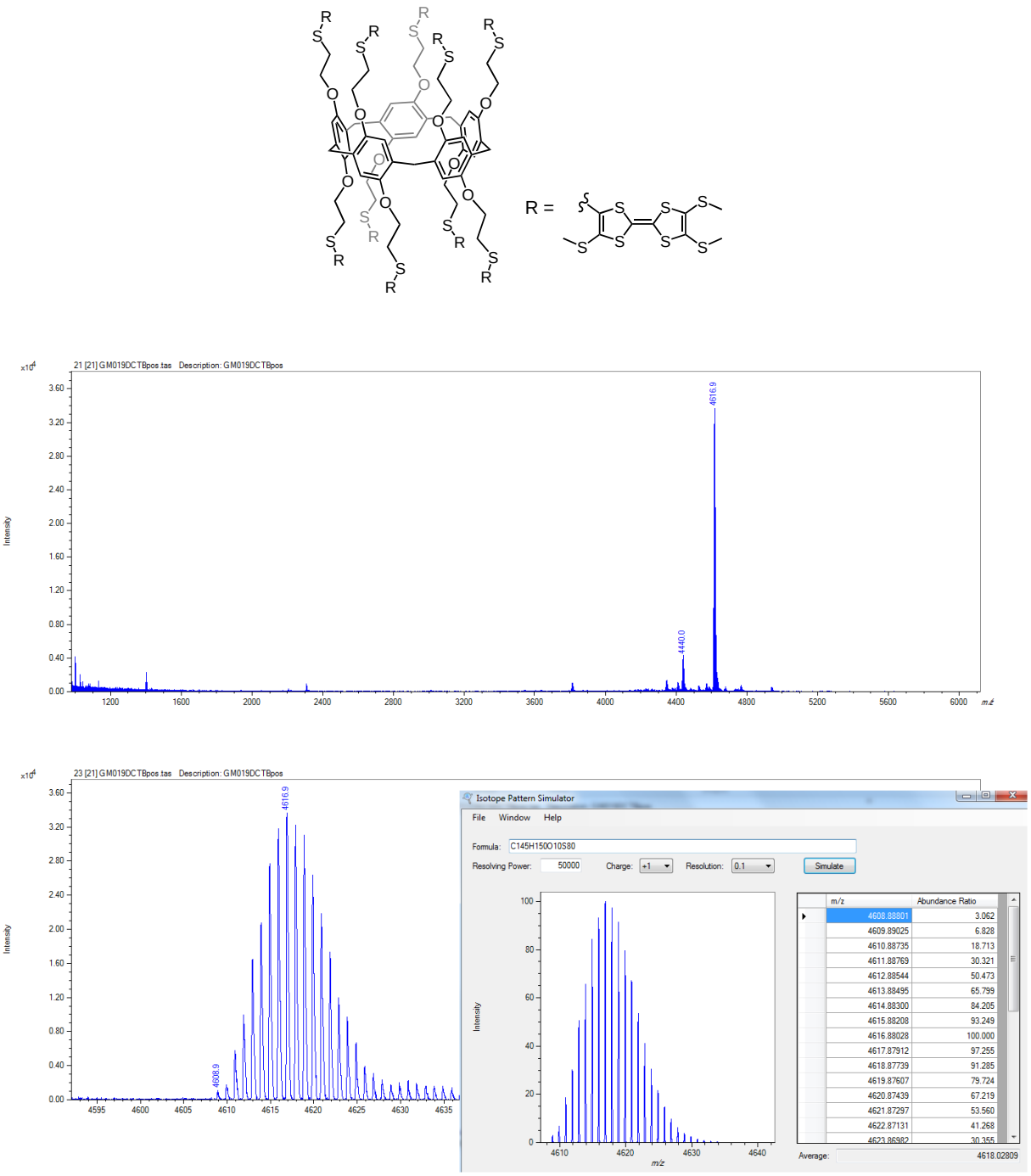

Figure S5d. MALDI-TOF mass spectrum of compound **3b**.

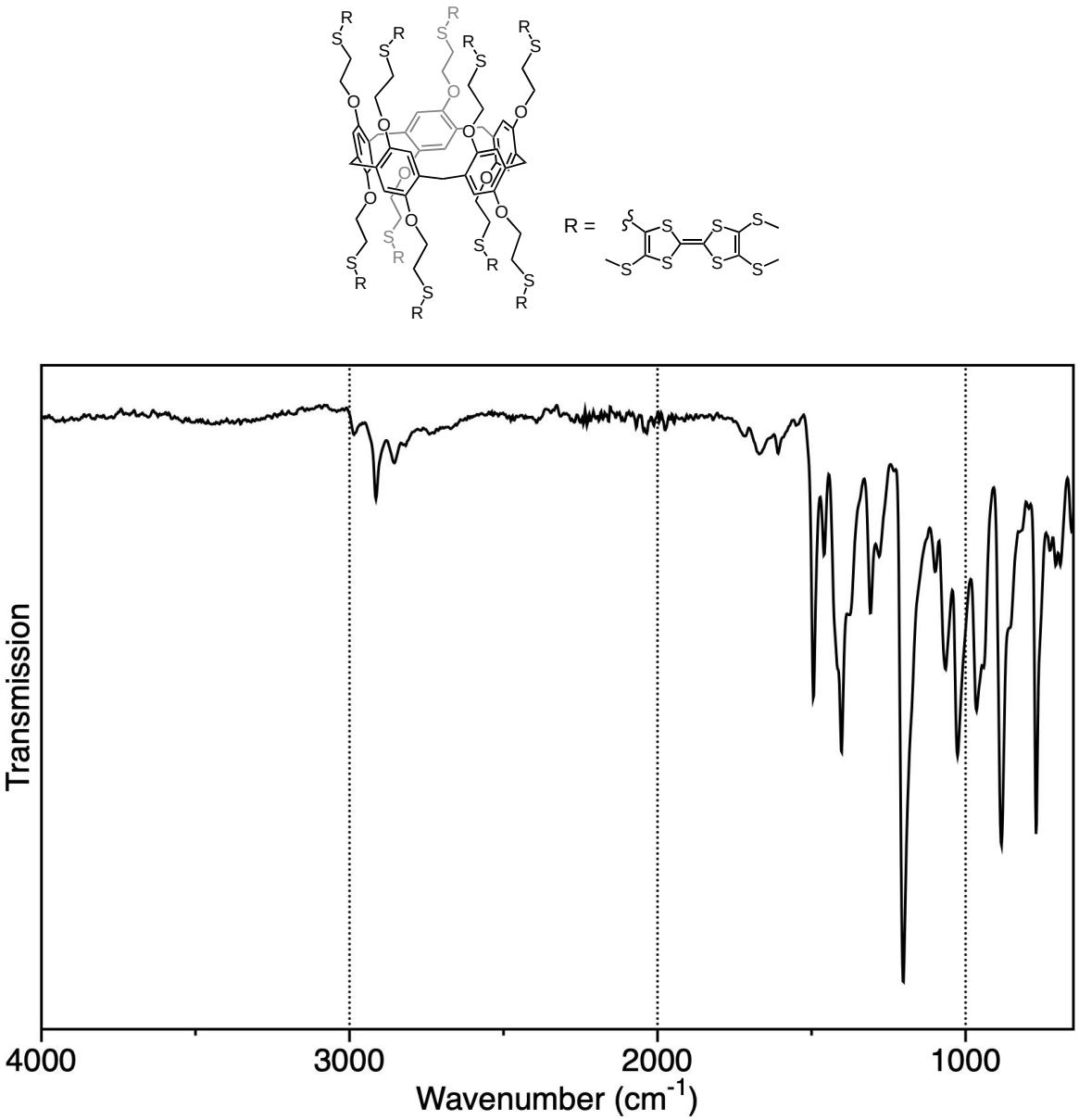

Figure S5e. IR spectrum of compound **3b**.

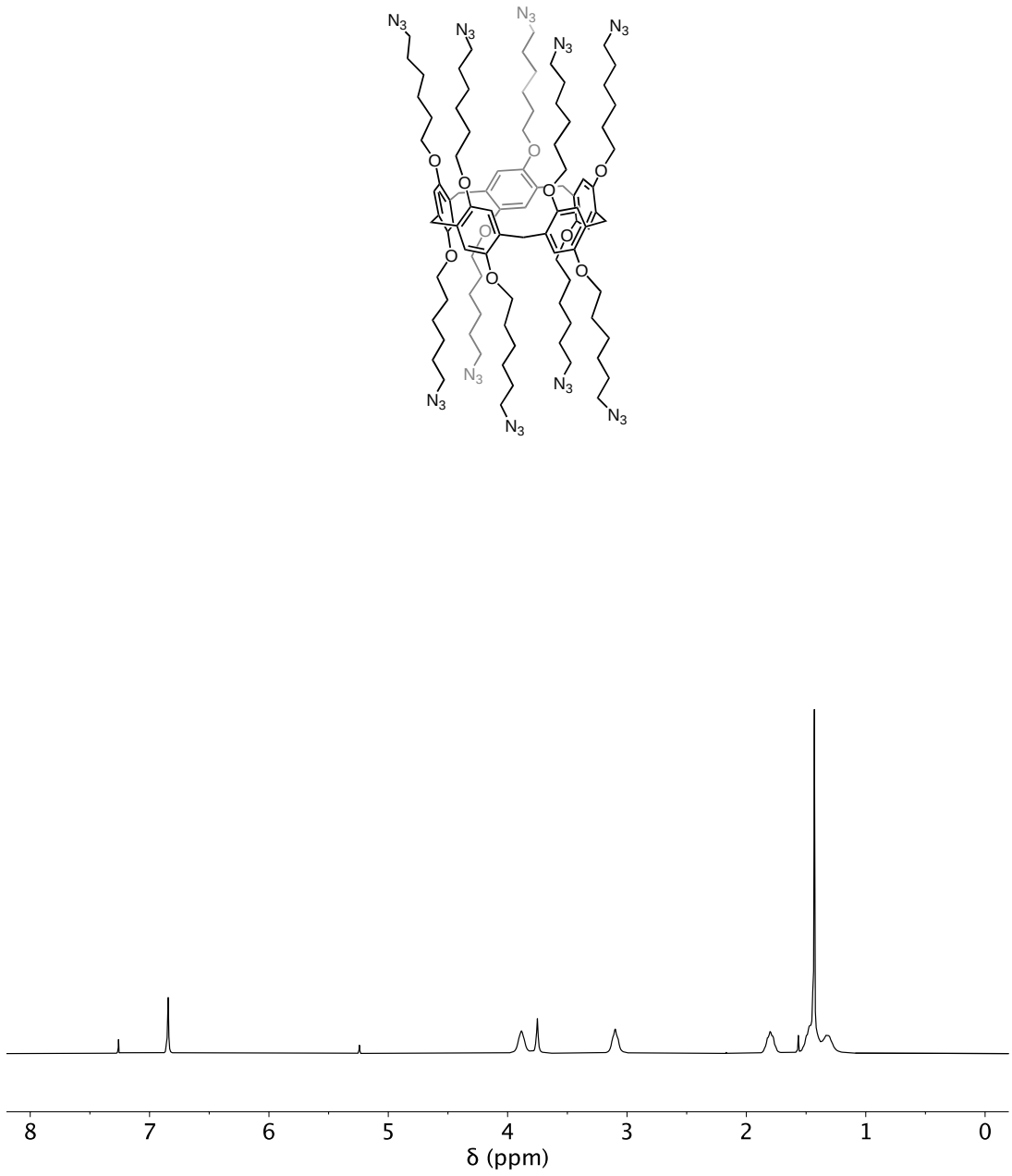

Figure S6a. ^{1}H NMR spectrum of compound **5** (300 MHz, $CDCl_3$, 298K).

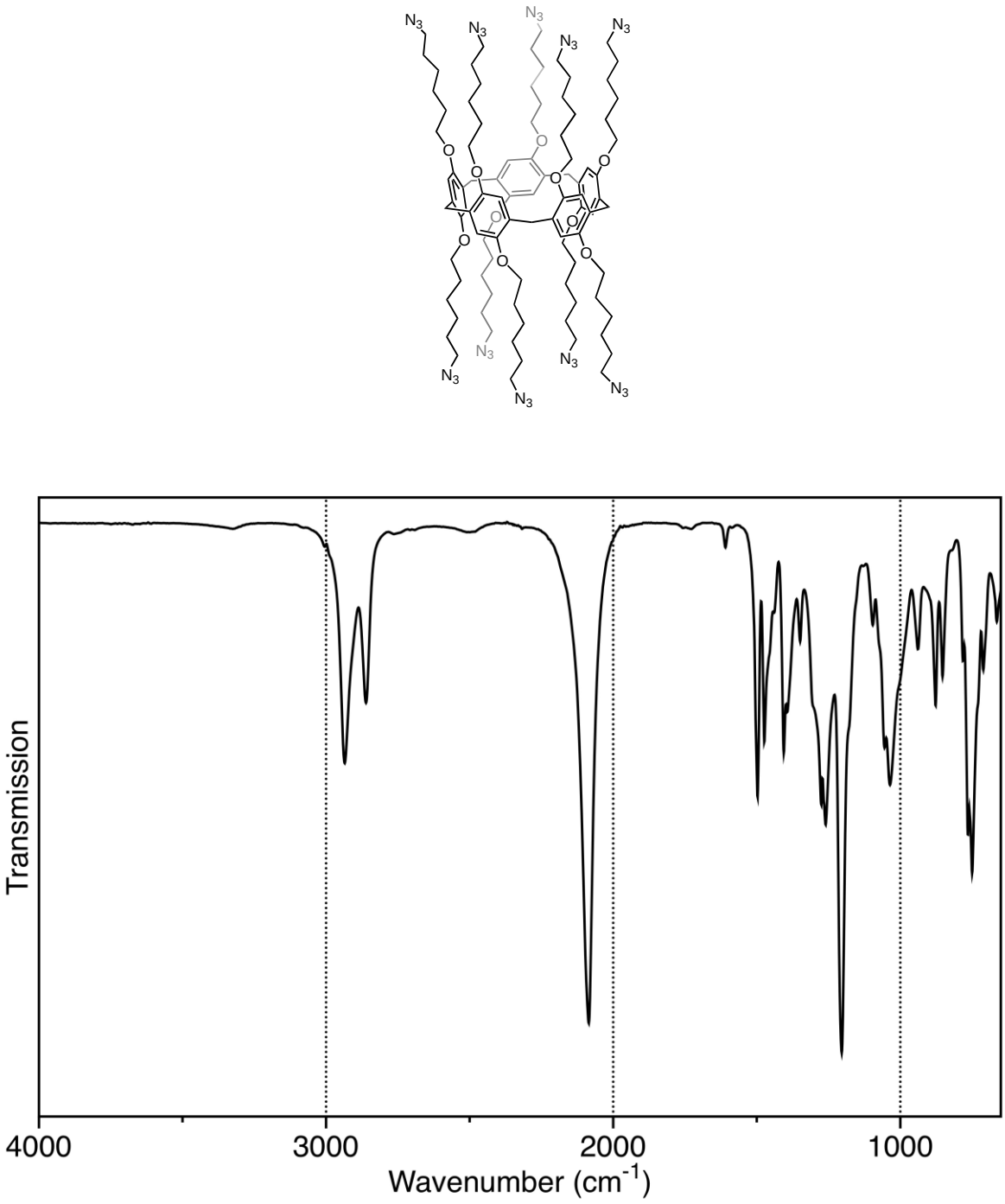

Figure S6b. IR spectrum of compound **5**.

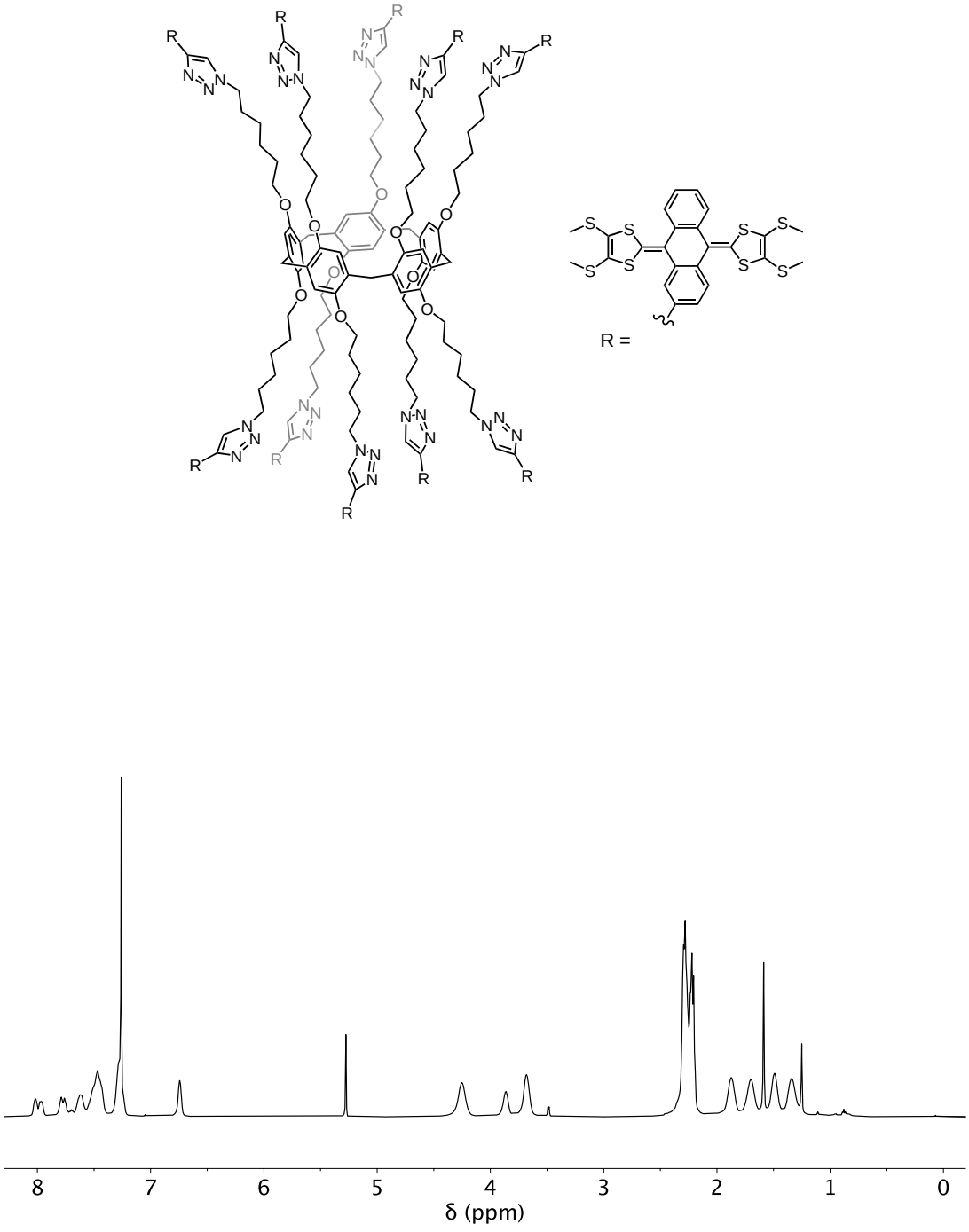

Figure S7a. ^{1}H NMR spectrum of compound **7** (500 MHz, $CDCl_3$, 298K).

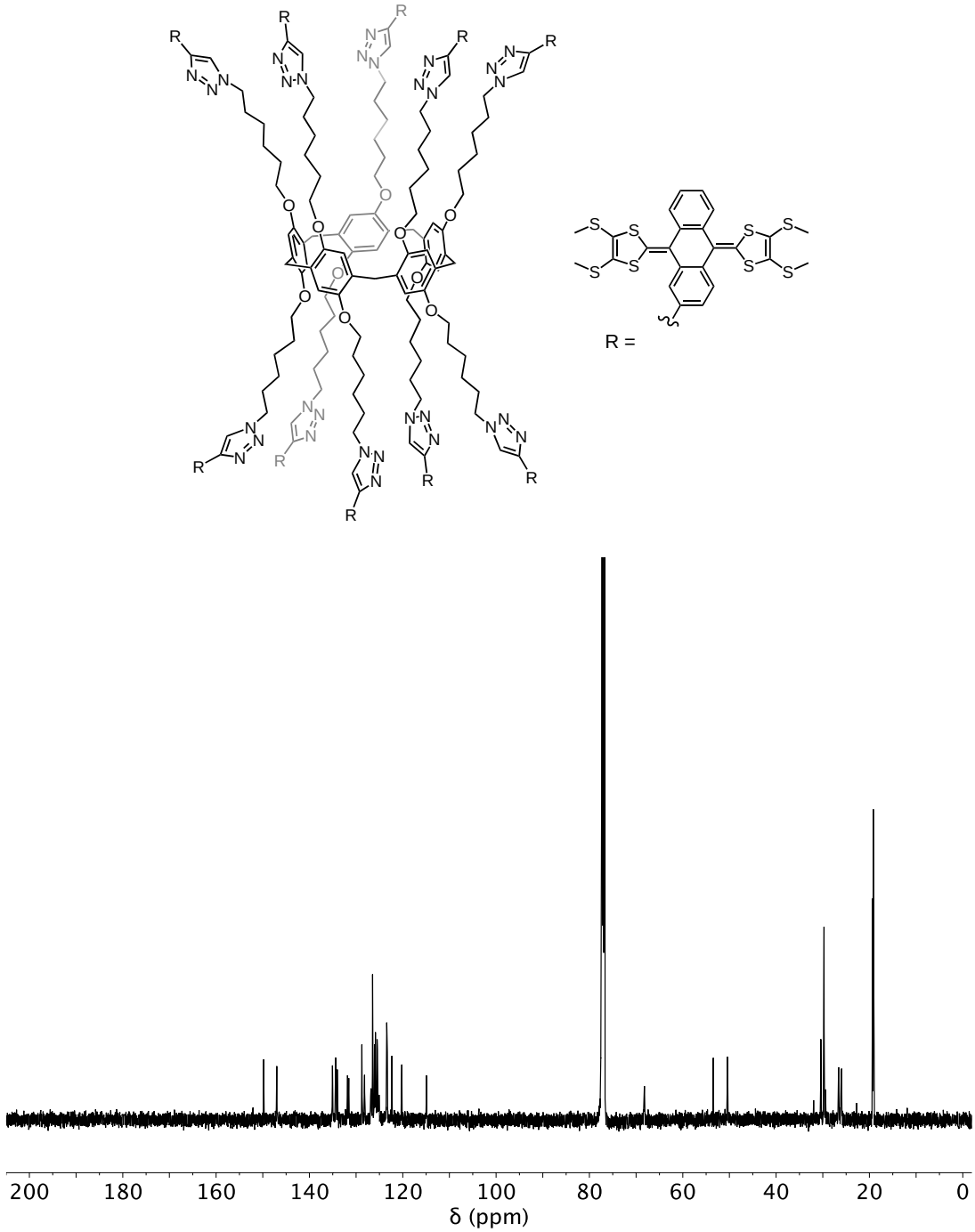

Figure S7b. ^{13}C NMR spectrum of compound **7** (125 MHz, $CDCl_3$, 298K).

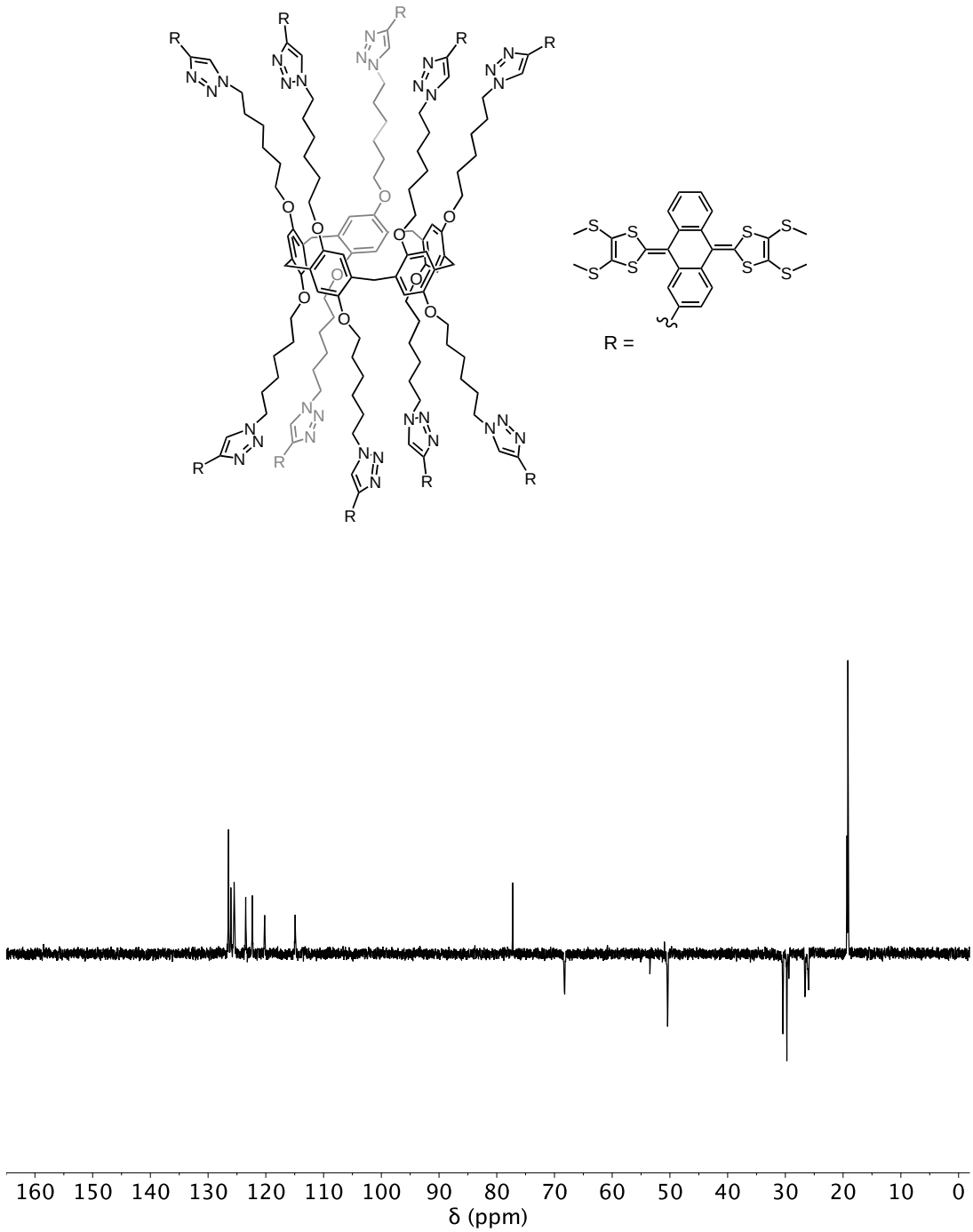

Figure S7c. DEPT spectrum of compound **7** (125 MHz, $CDCl_3$, 298K).

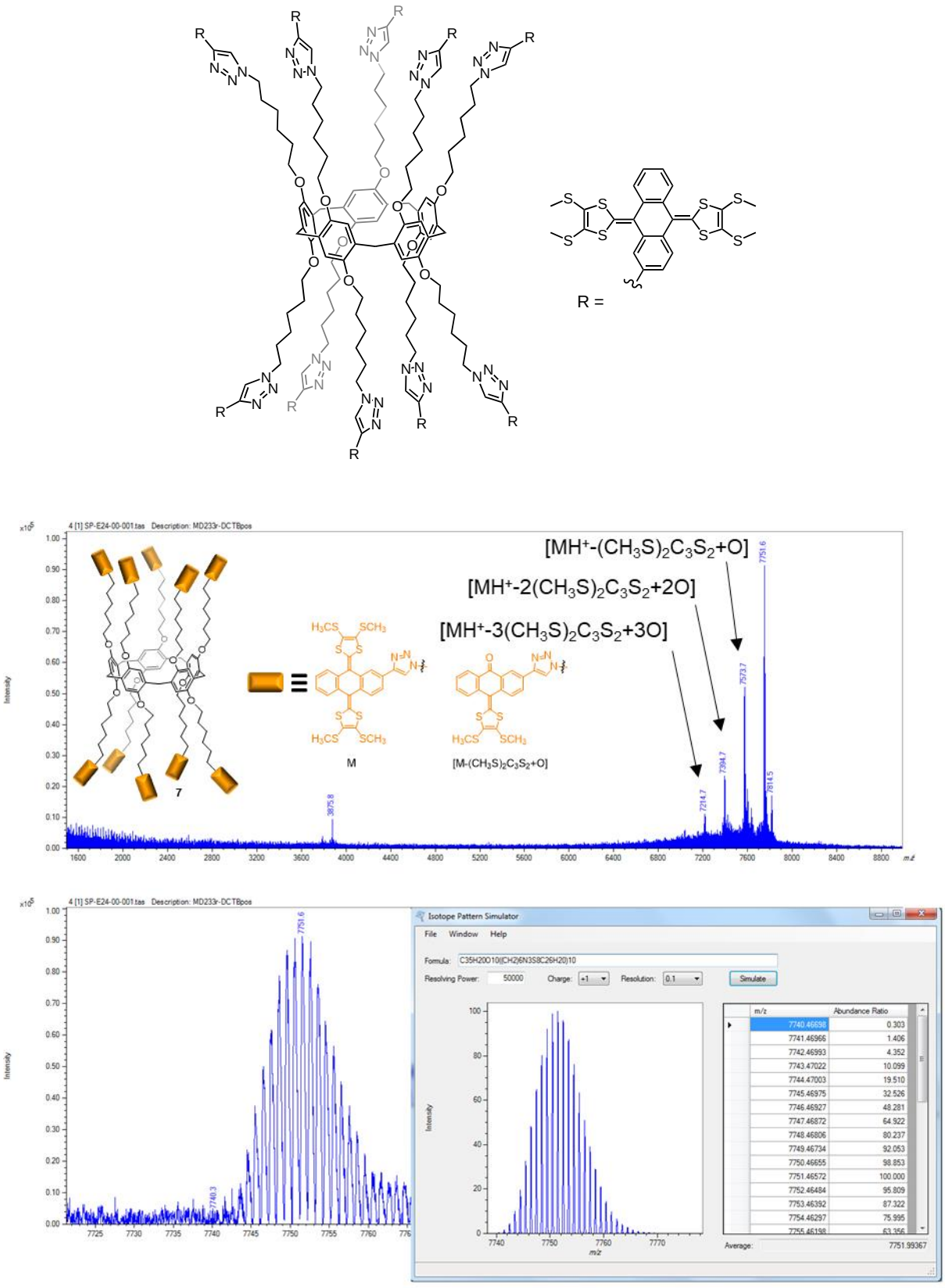

Figure S7d. MALDI-TOF mass spectrum of compound **7**.

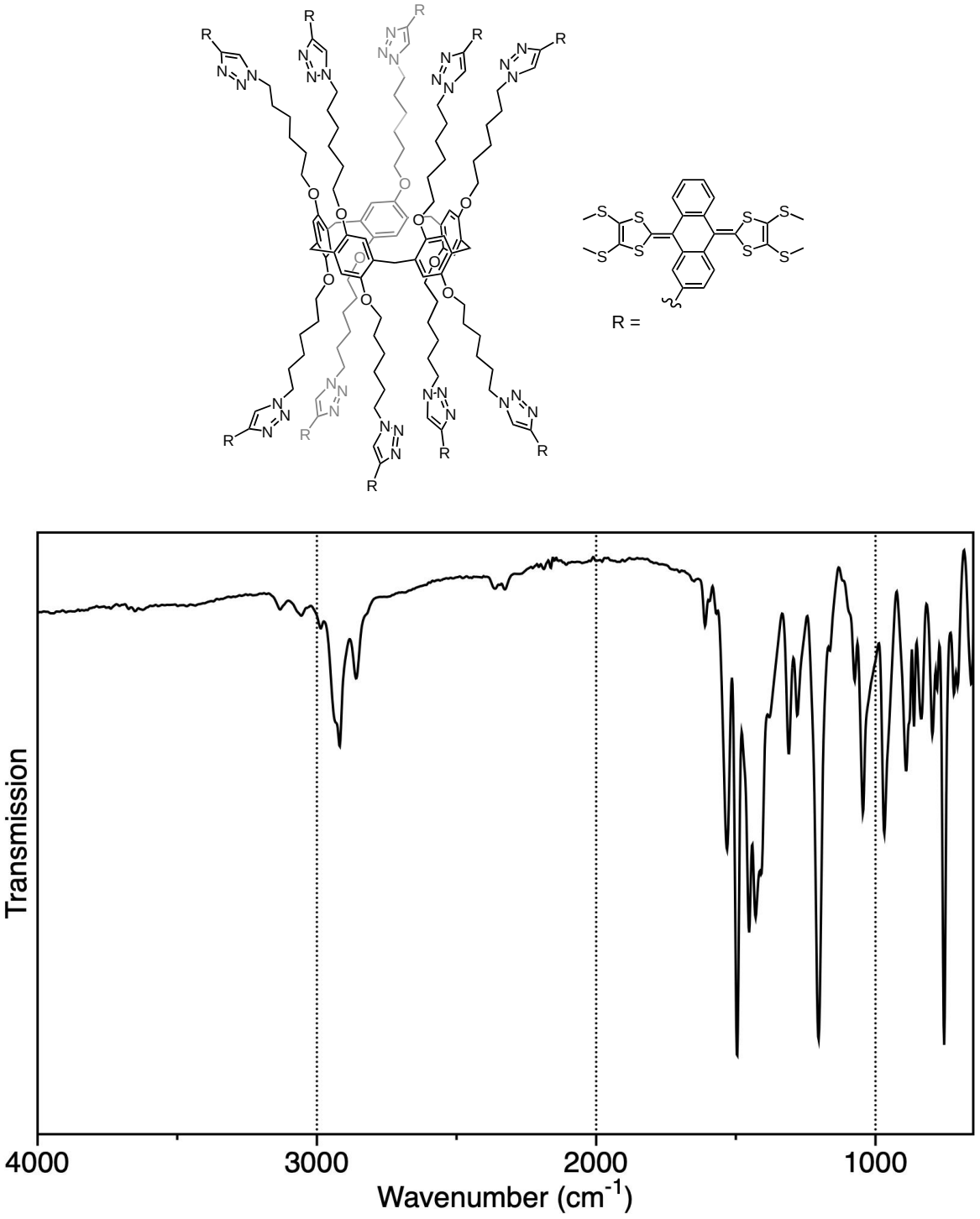

Figure S7e. IR spectrum of compound **7**.

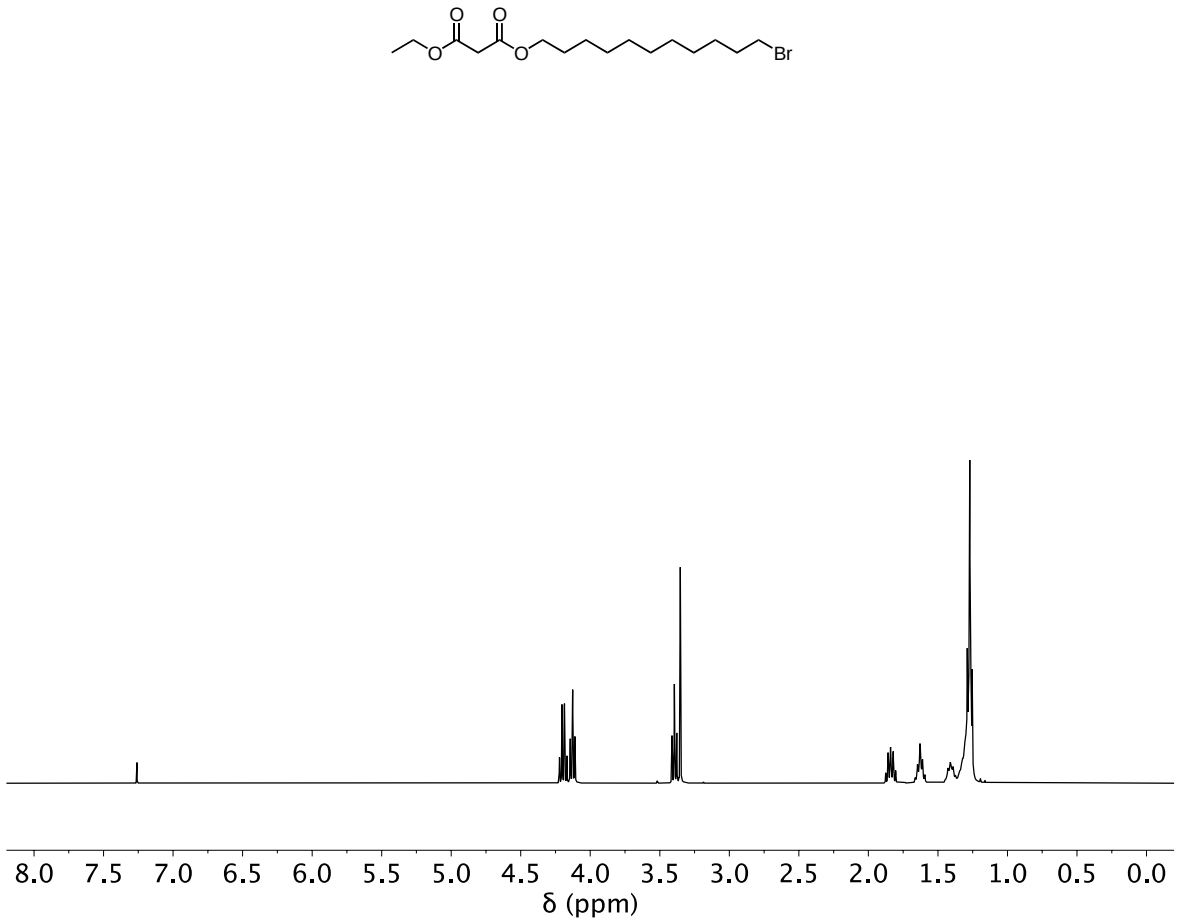

Figure S8a. ^{1}H NMR spectrum of compound **12** (400 MHz, $CDCl_3$, 298K).

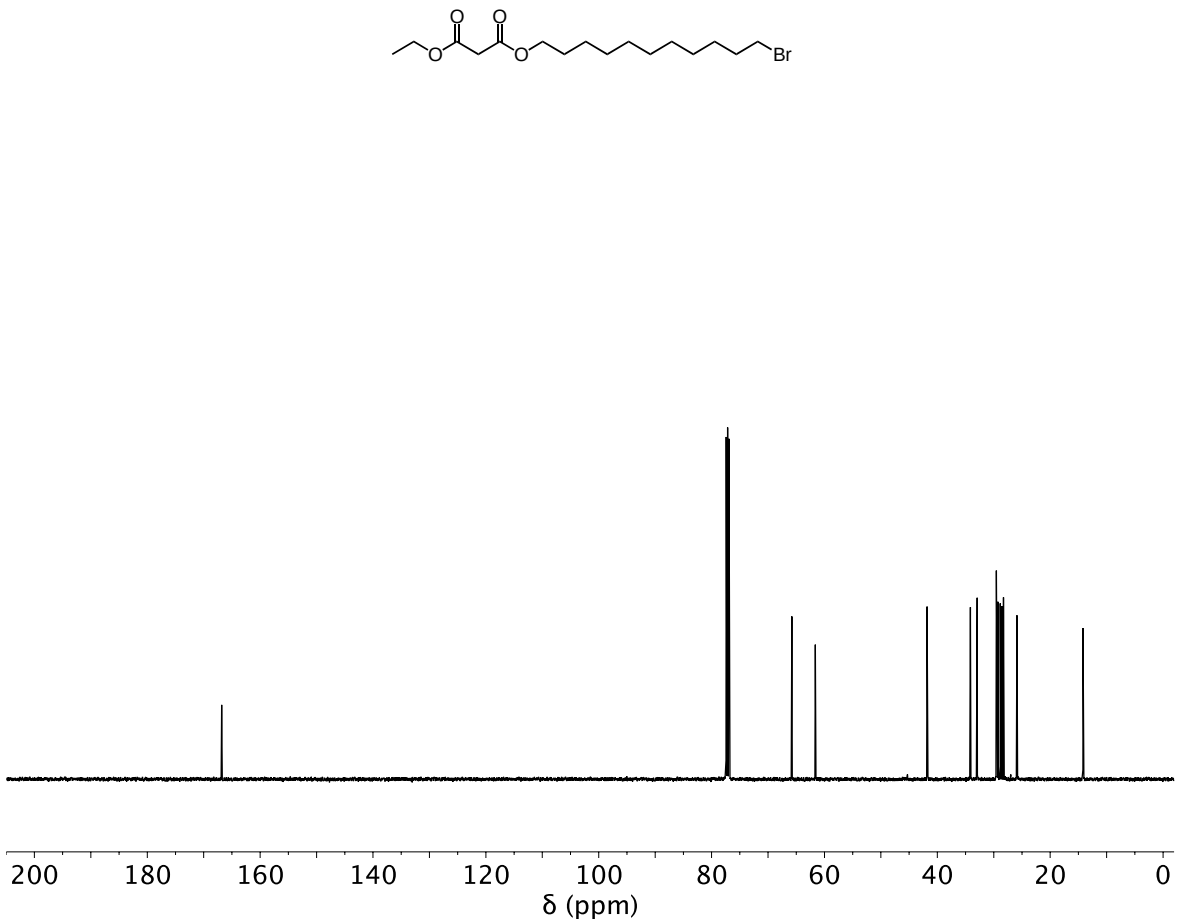

Figure S8b. ^{13}C NMR spectrum of compound **12** (125 MHz, $CDCl_3$, 298K).

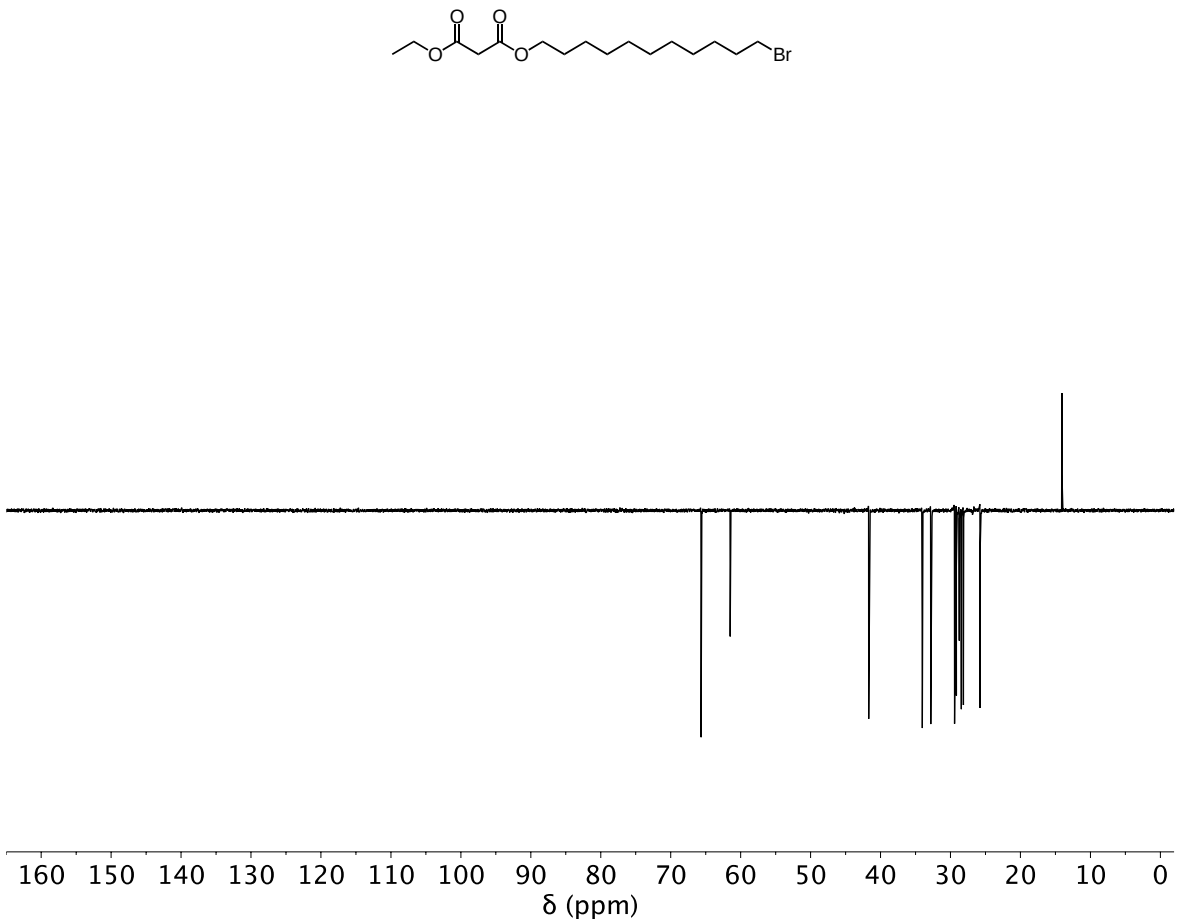

Figure S8c. DEPT spectrum of compound **12** (125 MHz, $CDCl_3$, 298K).

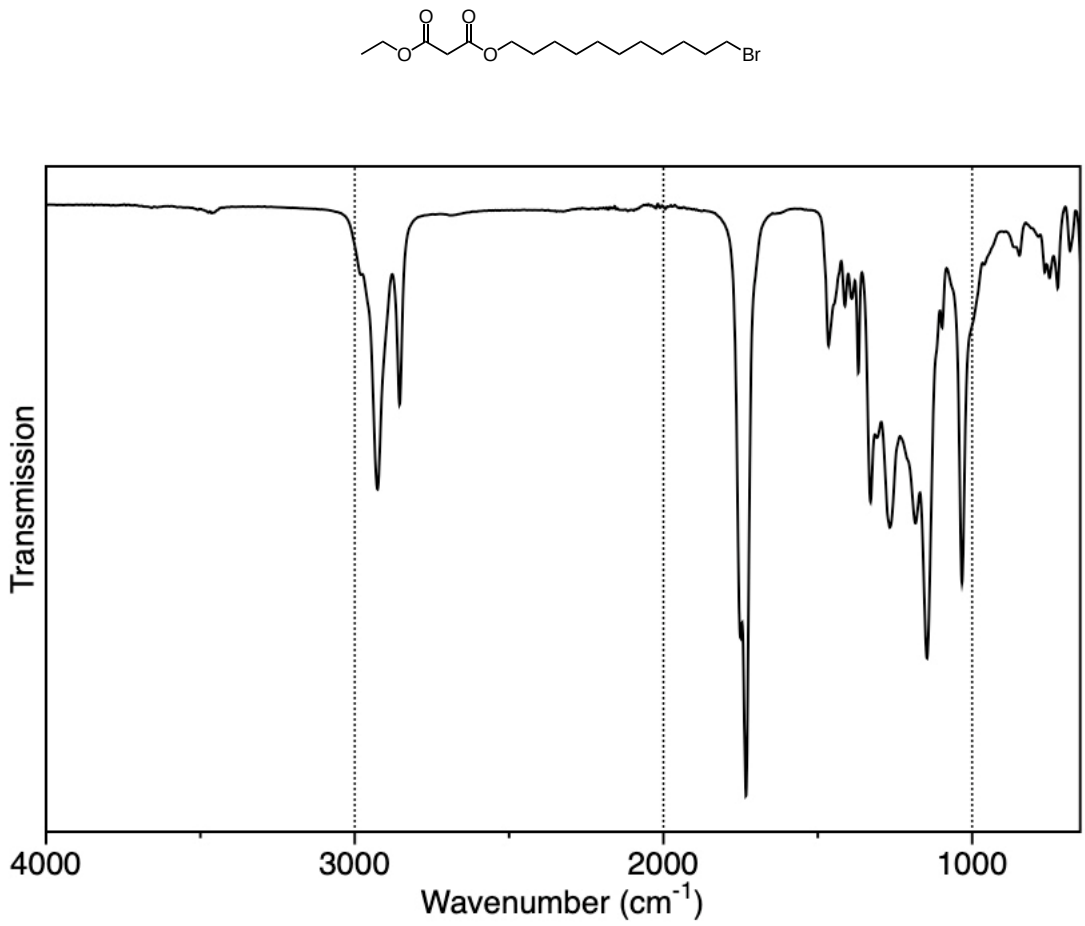

Figure S8d. IR spectrum of compound **12**.

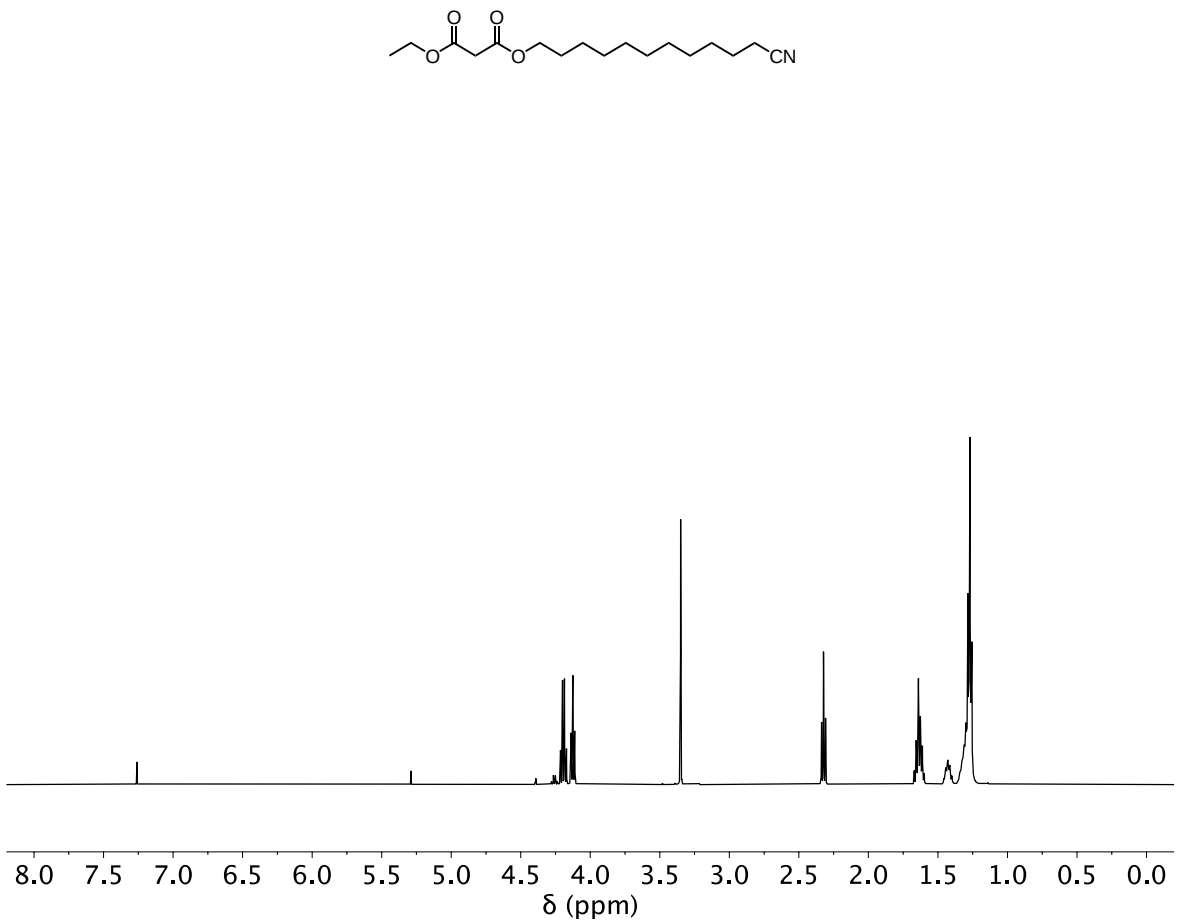

Figure S9a. ^{1}H NMR spectrum of compound **13** (500 MHz, $CDCl_3$, 298K).

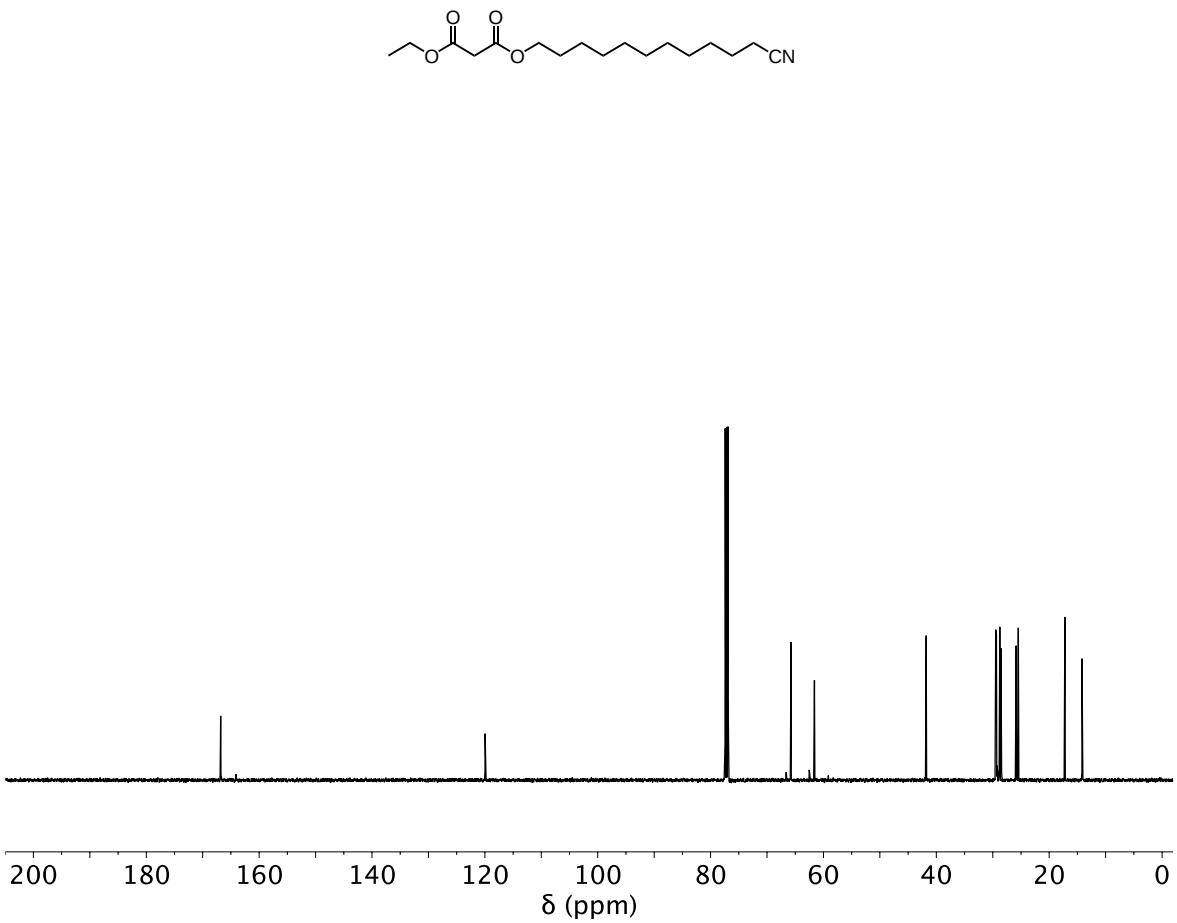

Figure S9b. ^{13}C NMR spectrum of compound **13** (125 MHz, $CDCl_3$, 298K).

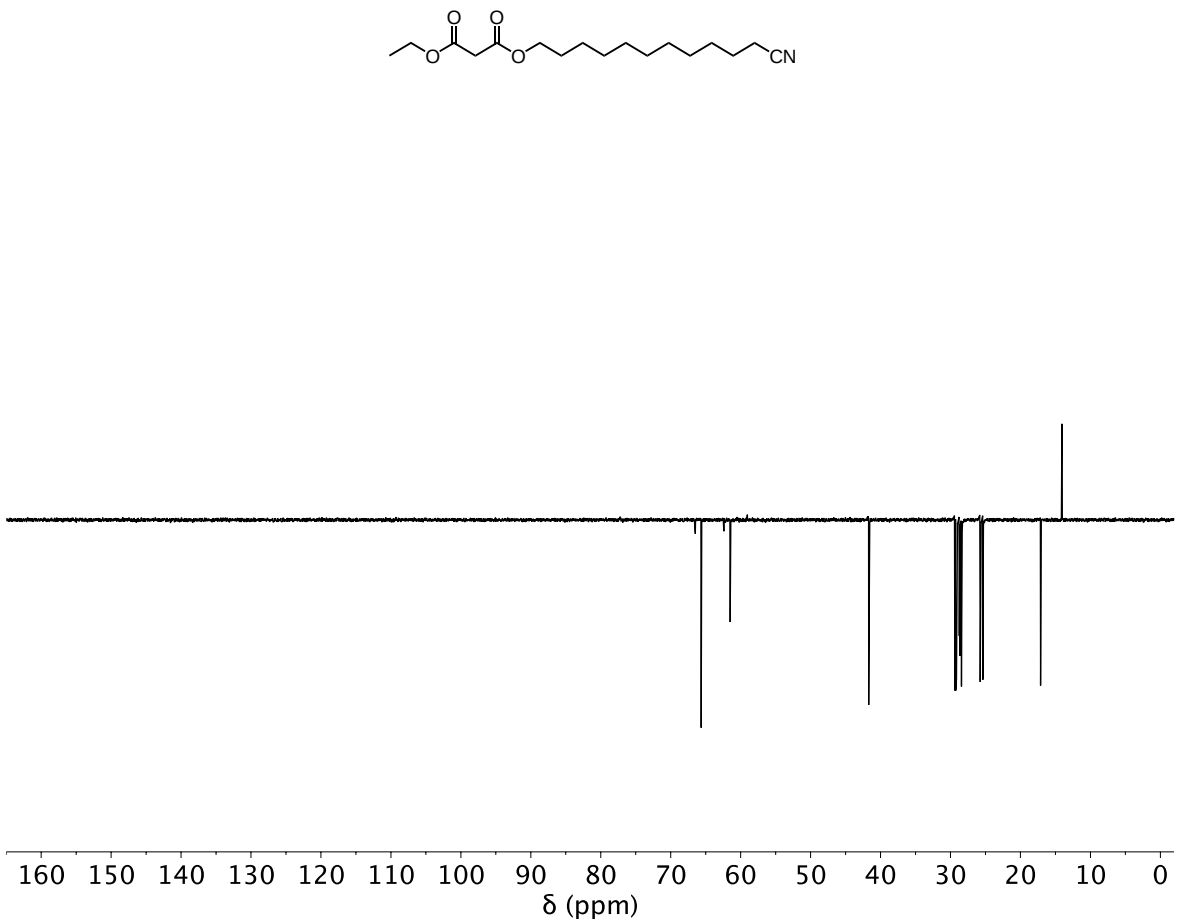

Figure S9c. DEPT spectrum of compound **13** (125 MHz, $CDCl_3$, 298K).

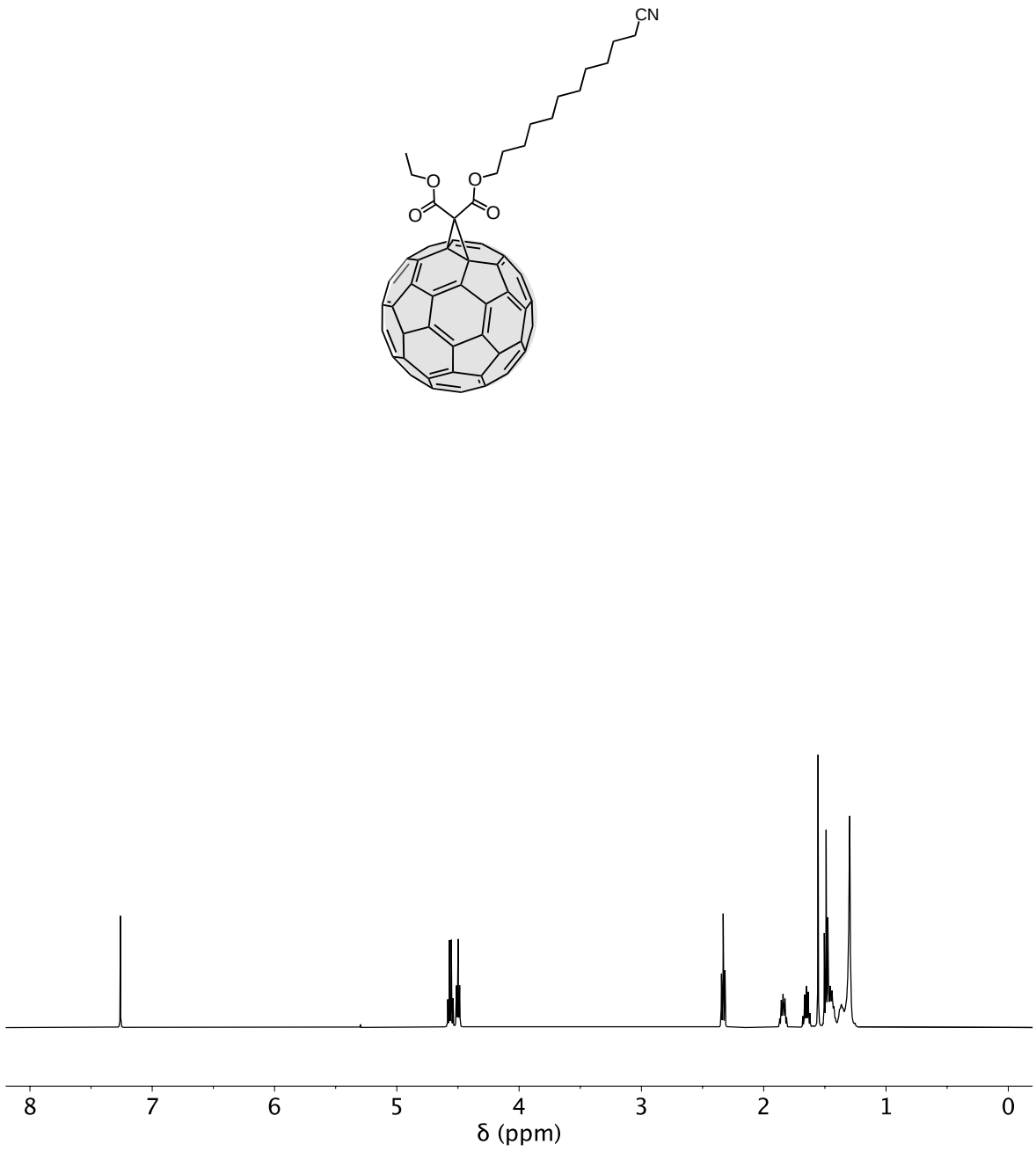

Figure S10a. ^{1}H NMR spectrum of compound **14** (500 MHz, $CDCl_3$, 298K).

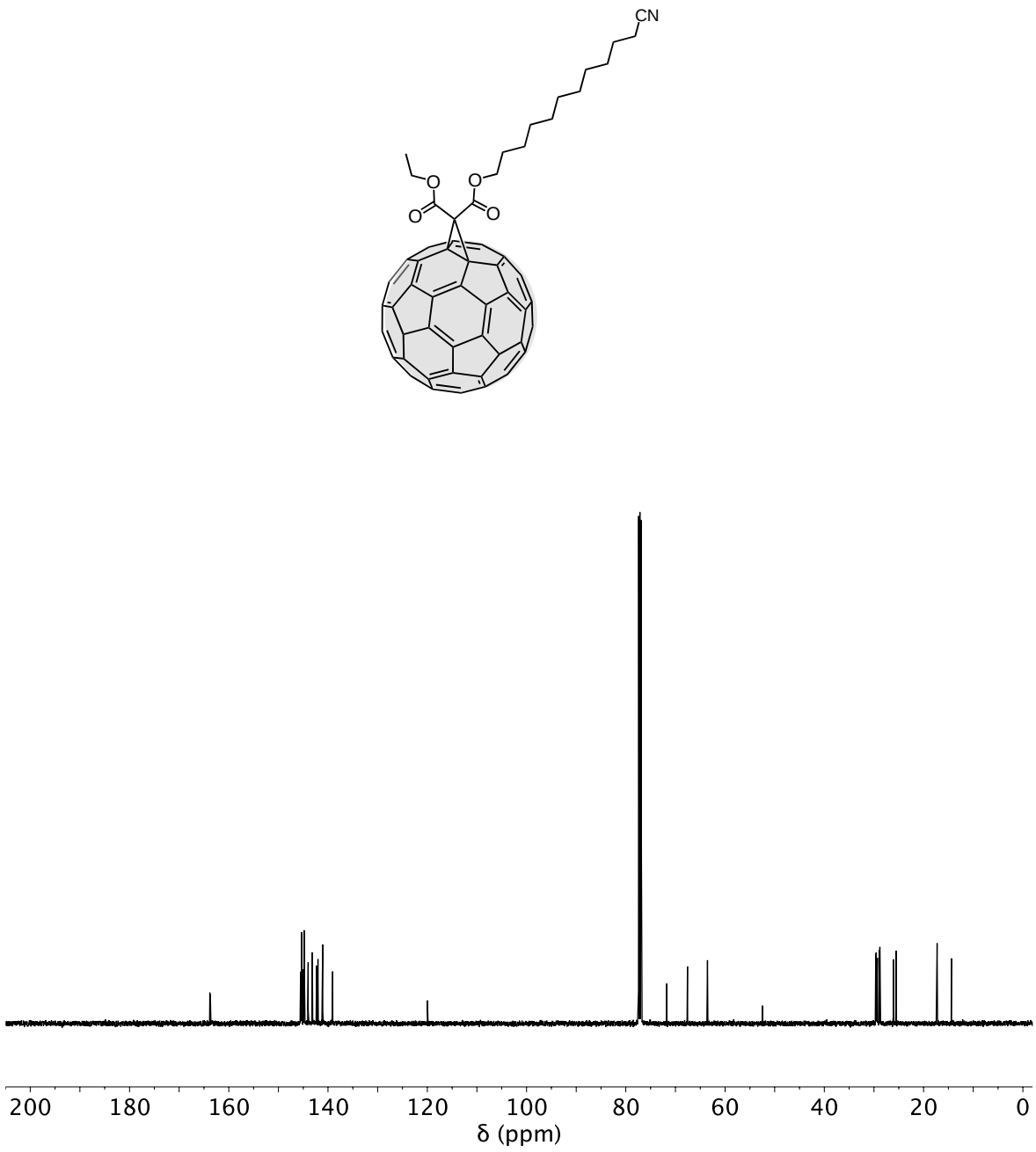

Figure S10b. ^{13}C NMR spectrum of compound **14** (125 MHz, $CDCl_3$, 298K).

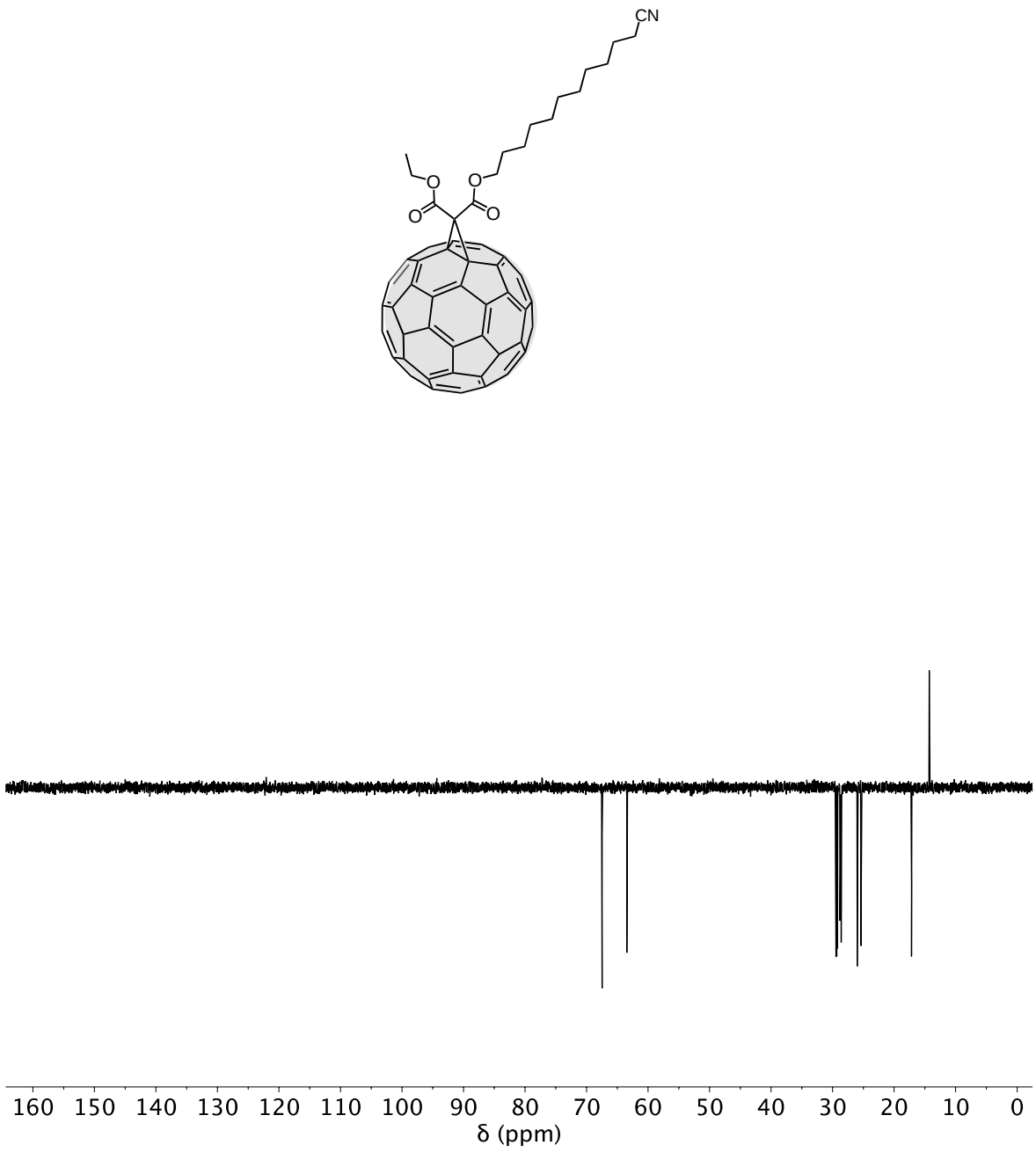

Figure S10c. DEPT spectrum of compound **14** (125 MHz, $CDCl_3$, 298K).

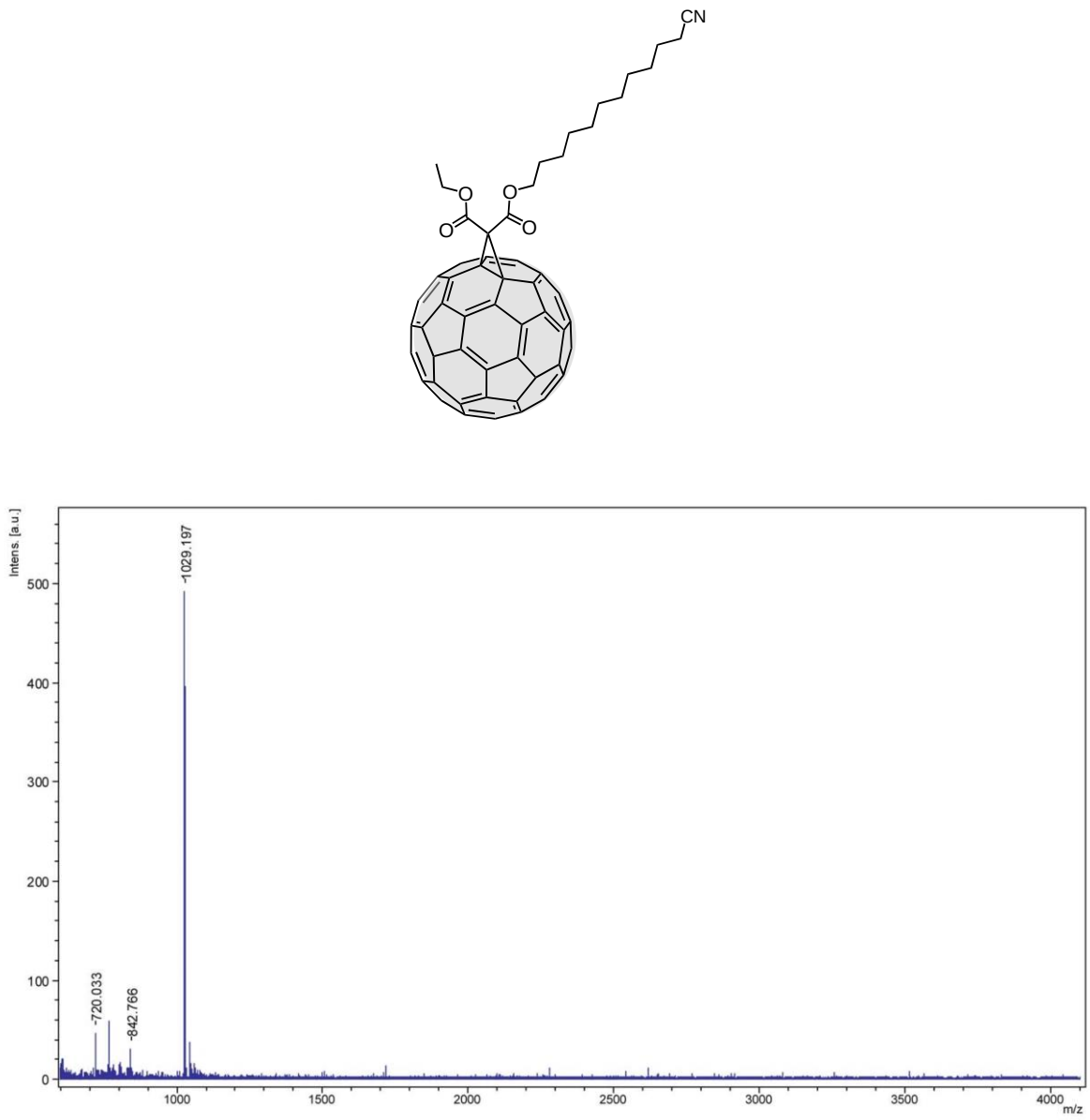

Figure S10d. MALDI-TOF mass spectrum of compound **14**.

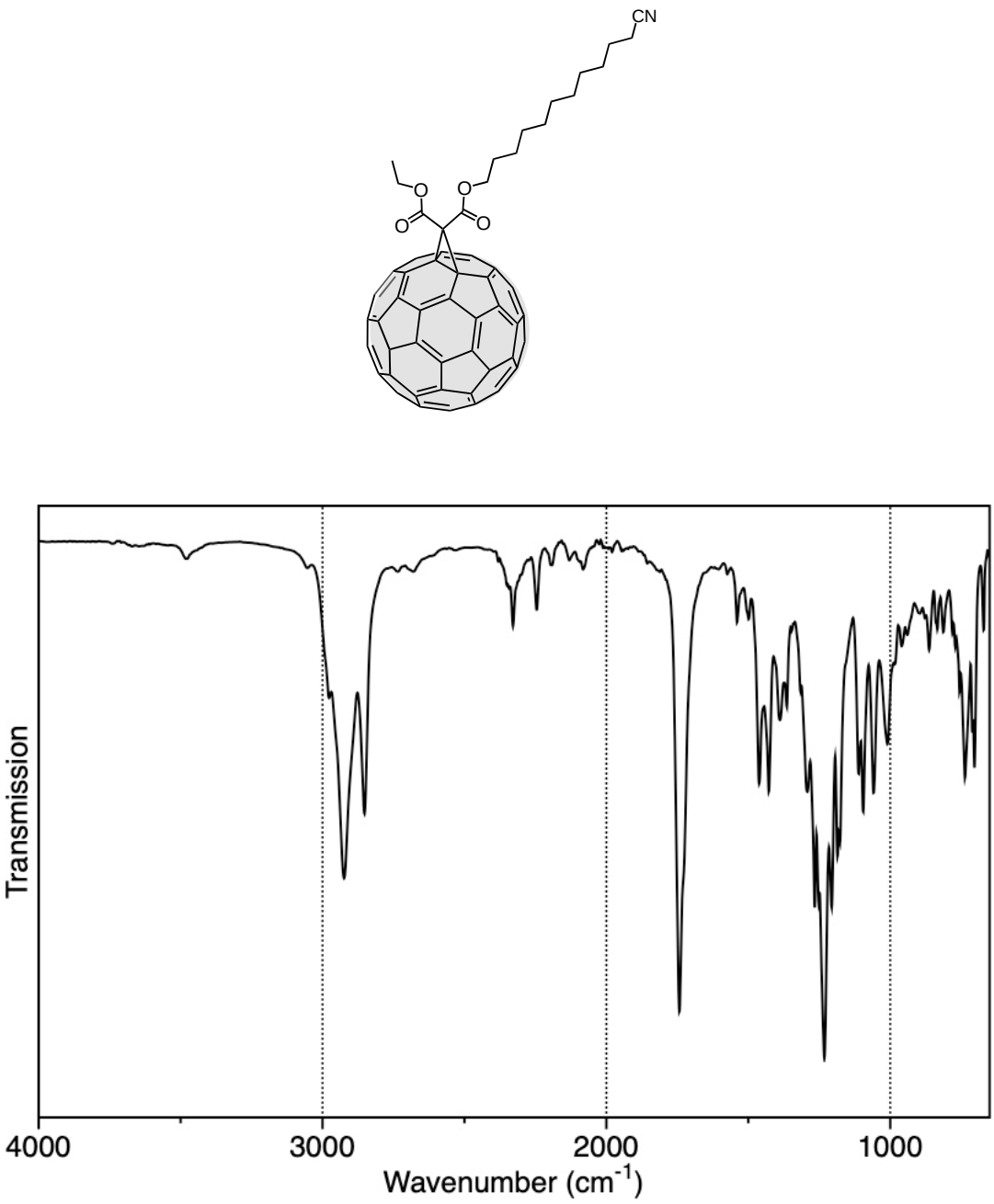

Figure S10e. IR spectrum of compound **14**.

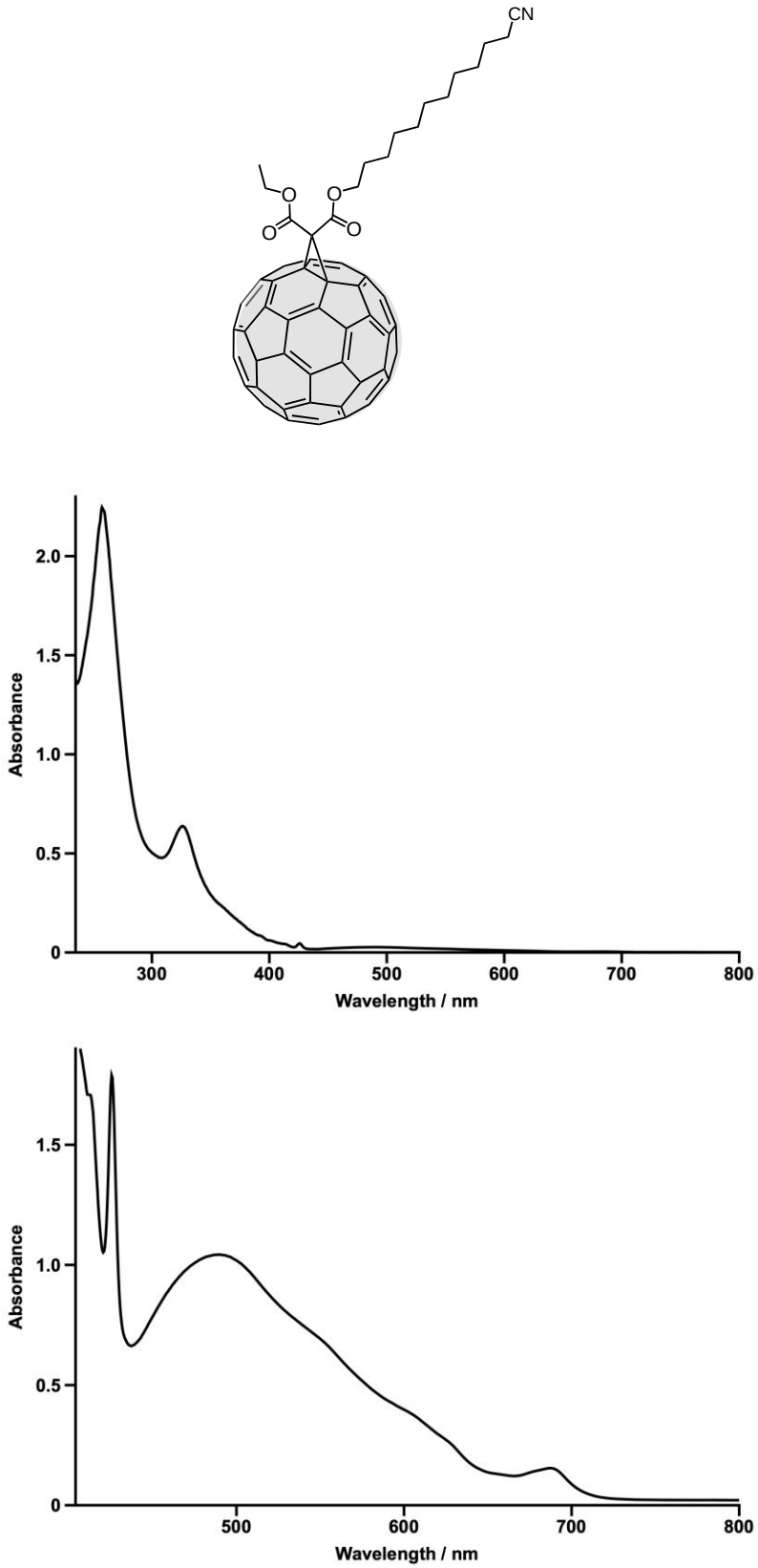

Figure S10f. UV/Vis spectra of compound **14** (CH_2Cl_2, 298K, d = 1 cm, top: $C_M = 1.57\times10^{-5}$ M; bottom: $C_M = 6.31\times10^{-4}$ M).

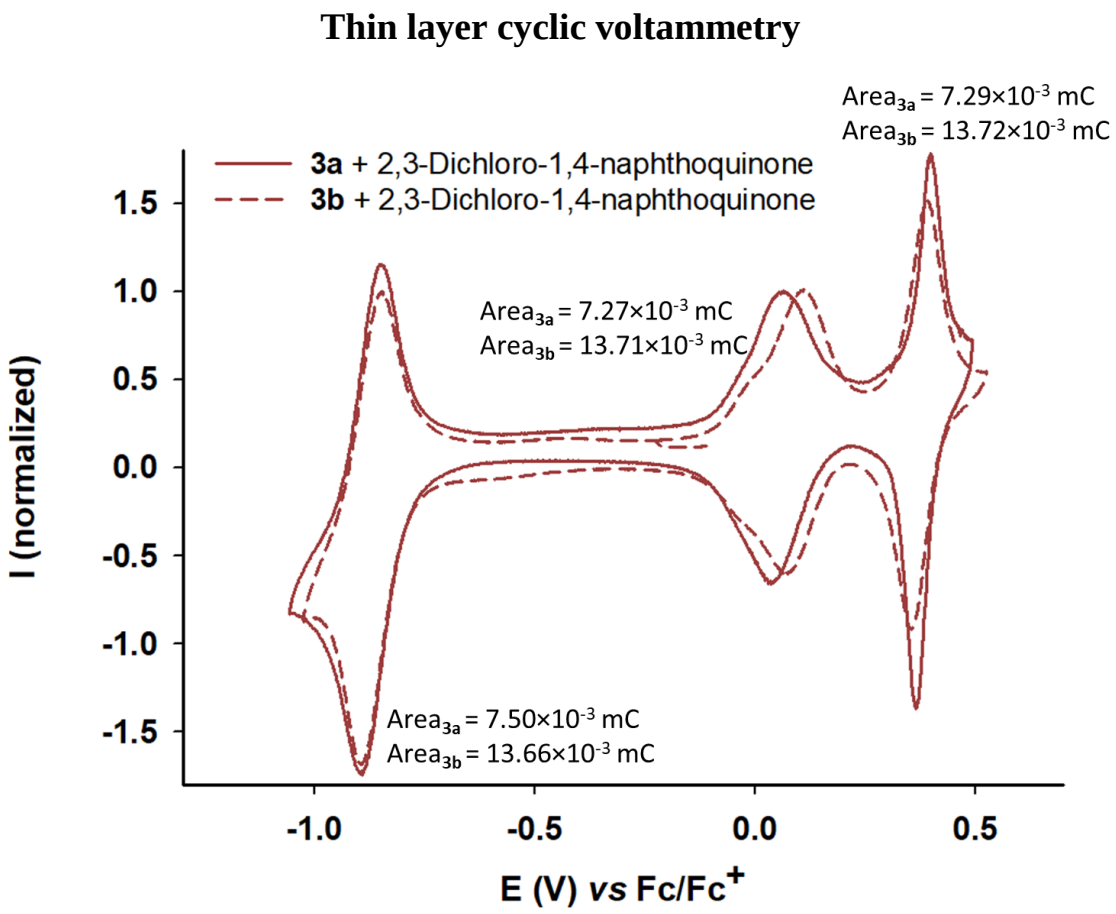

Figure S11. Thin Layer Cyclic Voltammetry of compounds **3a** and **3b** (C = 2.5×10^{-4} M, CH_2Cl_2:CH_3CN, 90:10 for **3a** and 75:25 for **3b**, $C_{Dichlon} = 2.5\times10^{-3}$ M, 0.1 M nBu$_4$NPF$_6$, v = 10 mV·s^{-1}, Pt), E *vs* Fc/Fc$^+$.

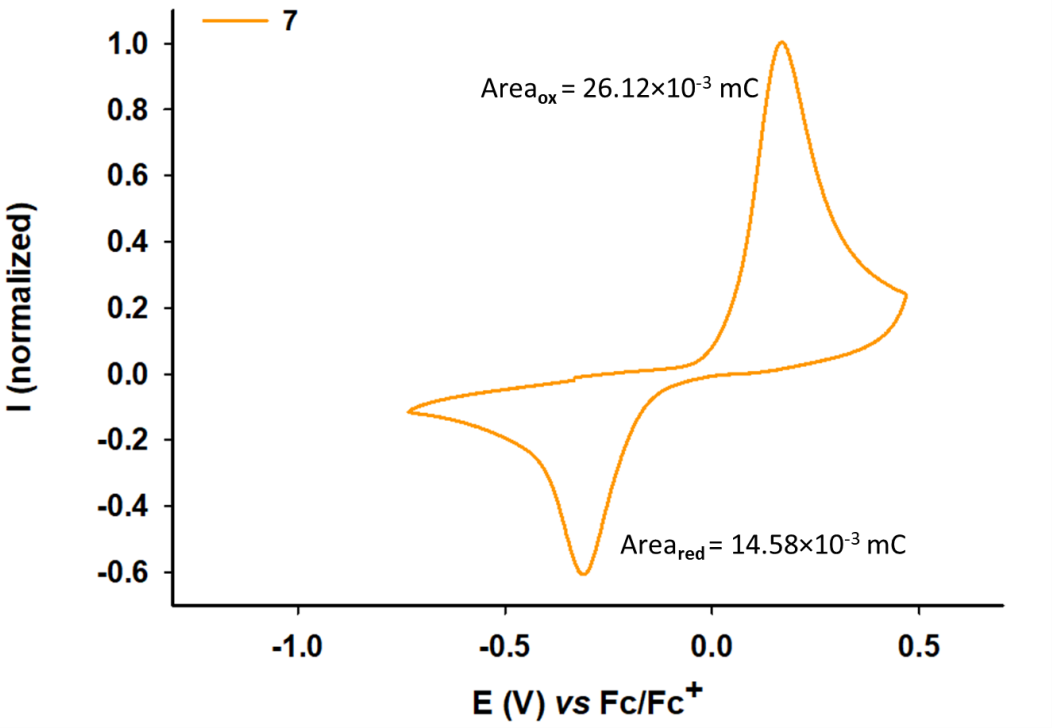

Figure S12. Cyclic Voltammetry of compound **7** (C = 2.5×10^{-4} M, CH_2Cl_2, 0.1 M *n*Bu_4NPF_6, v = 100 mV·s^{-1}, Pt), E *vs* Fc/Fc^{+}.

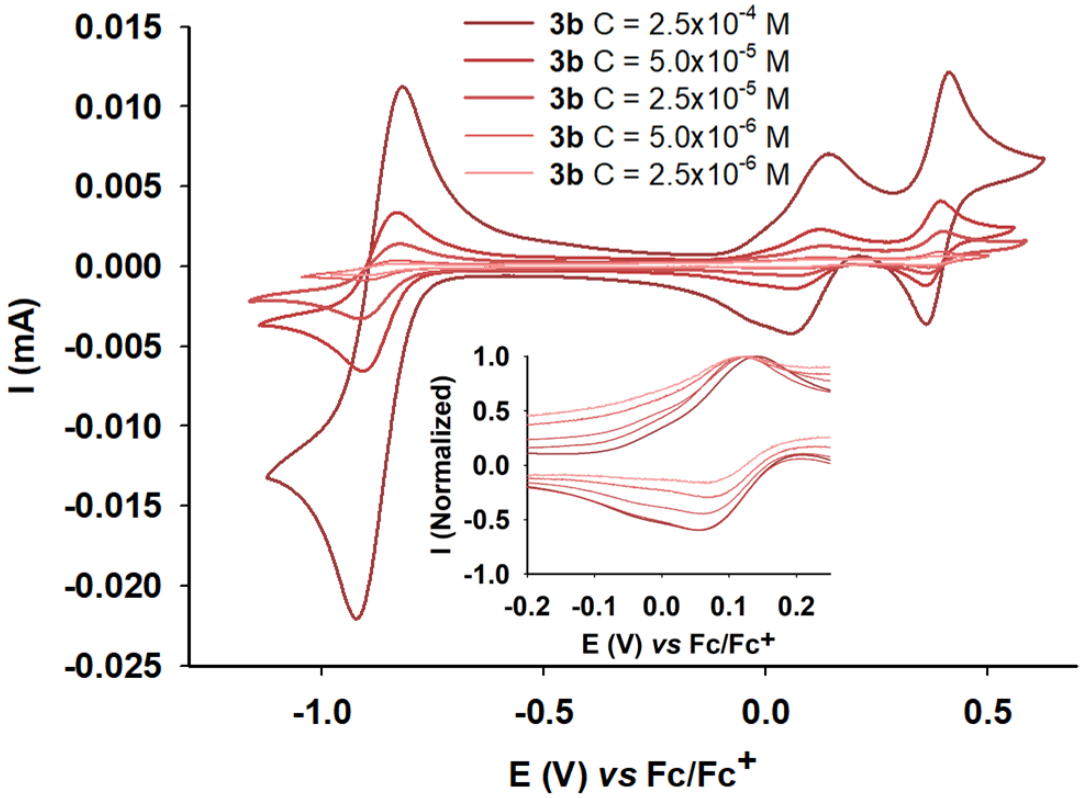

Figure S13. Cyclic Voltammetry of compound **3b** (C = 2.5×10^{-4} M, CH_2Cl_2:CH_3CN, 75:25), diffusion regime, in presence of 10 equiv. of 2,3-dichloro-1,4-naphthoquinone, v = 100 $mV.s^{-1}$.

^{1}H NMR titration experiments

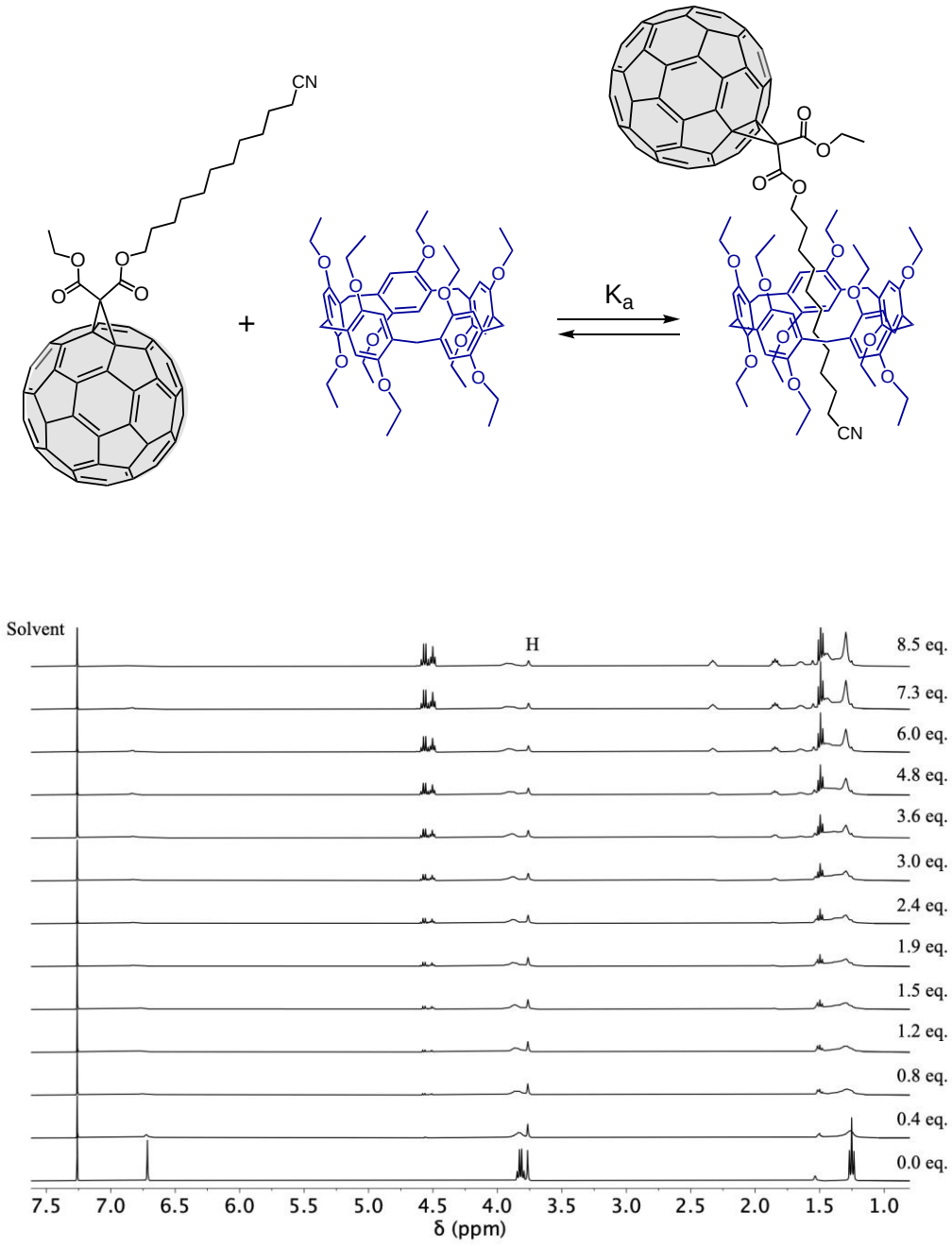

Figure S14a. ^{1}H NMR spectra (400 MHz, $CDCl_3$, 298K) recorded upon successive additions of guest **14** to a solution of host **8** (3.8 mM).

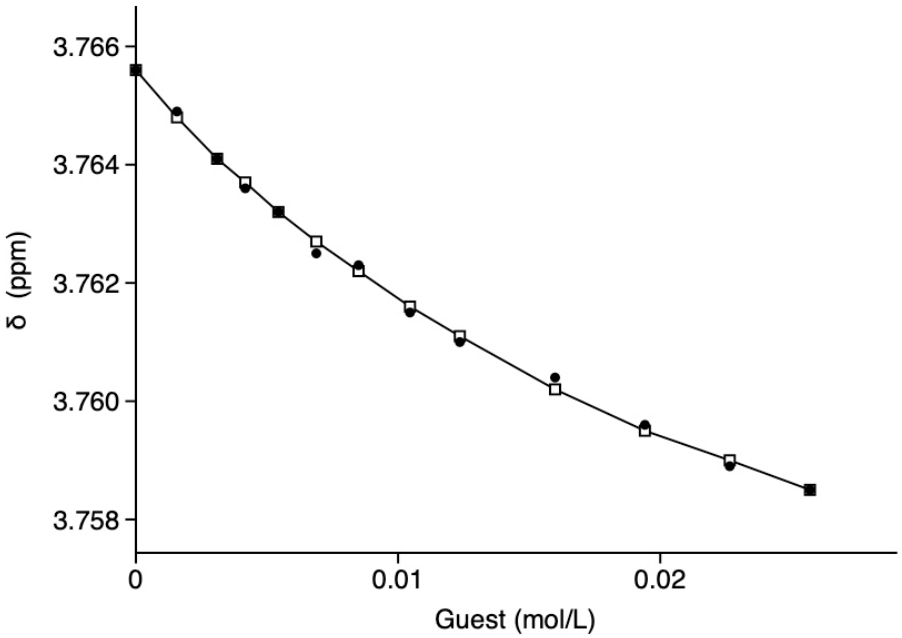

Fig. S14b. Chemical shifts of H (**8**, calculated: □, experimental: ●) as a function of guest concentration.

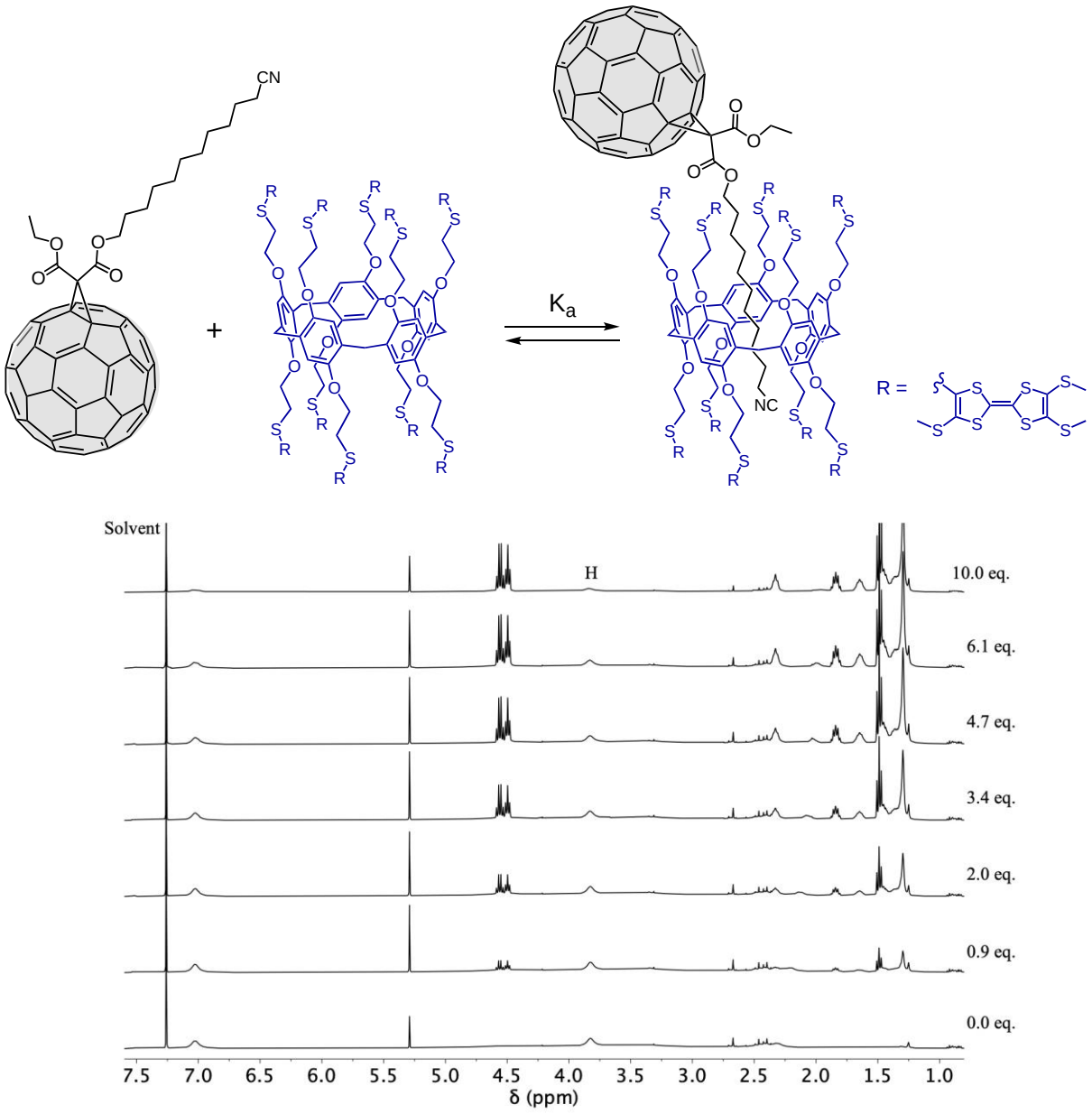

Figure S15a. Selected ^{1}H NMR spectra (400 MHz, $CDCl_3$, 298K) recorded upon successive additions of guest **14** to a solution of host **3b** (4 mM).

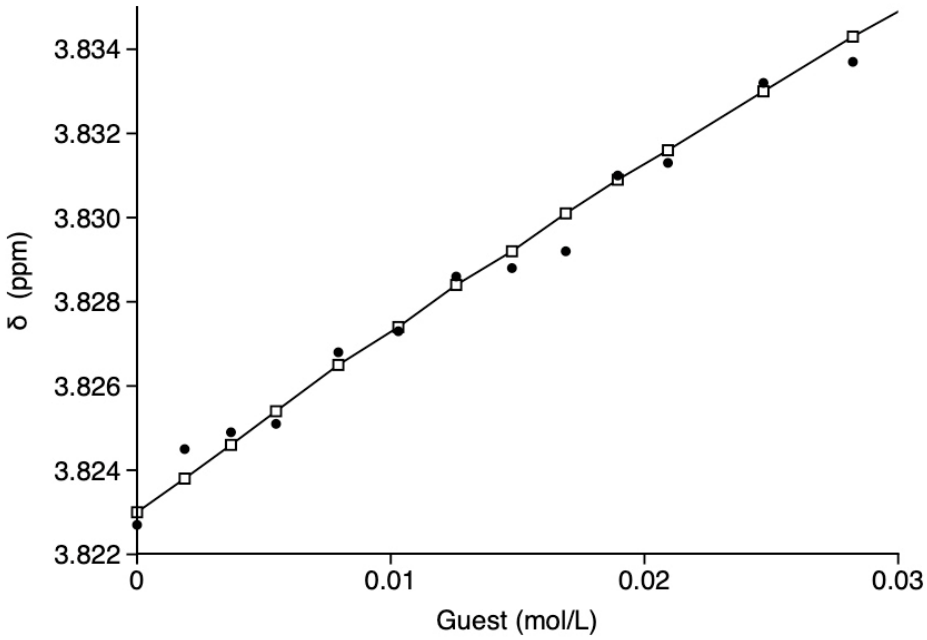

Fig. S15b. Chemical shifts of H_A (**3b**, calculated: □, experimental: ●) as a function of guest concentration.

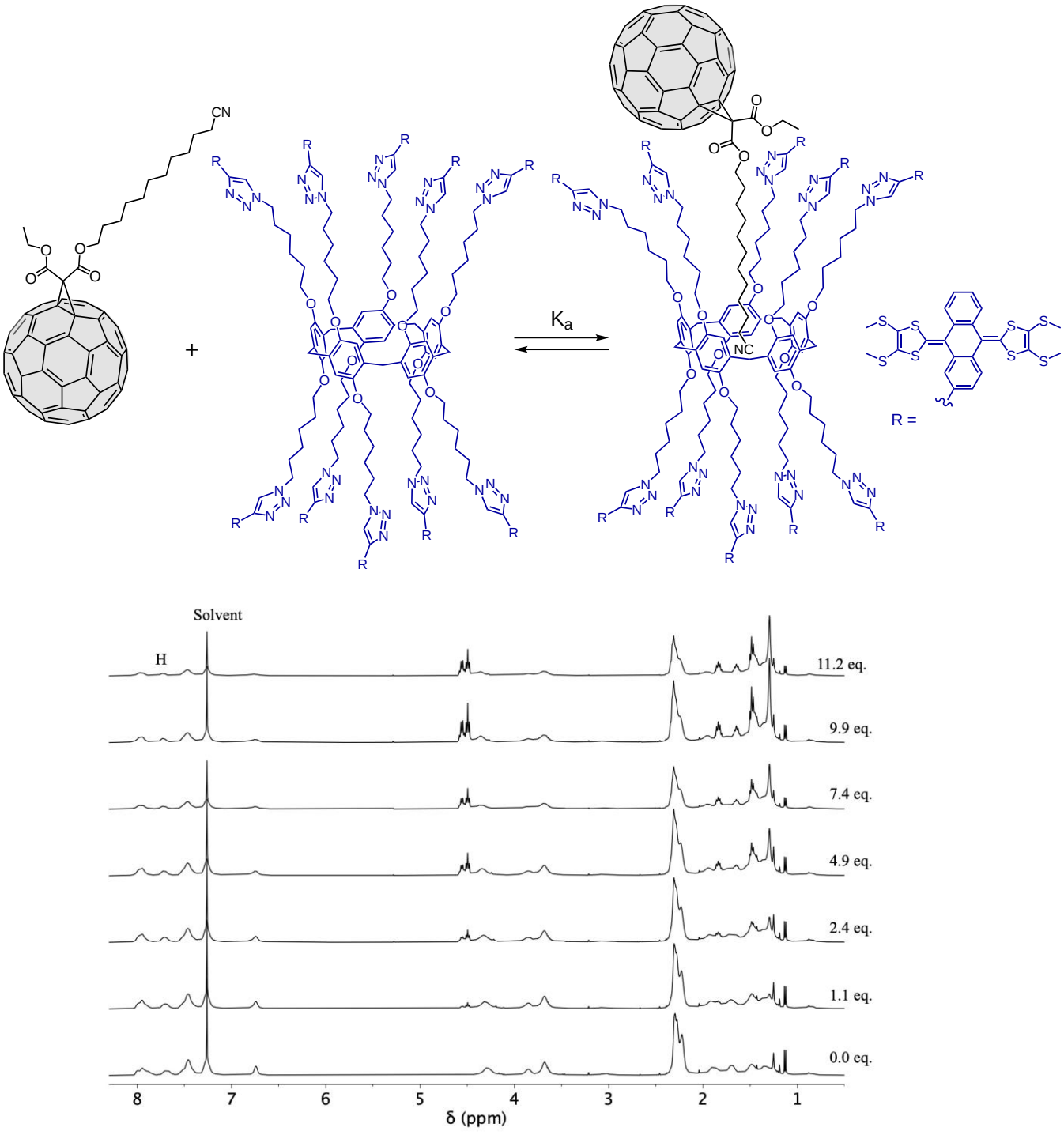

Figure S16a. Selected ^{1}H NMR spectra (400 MHz, $CDCl_3$, 298K) recorded upon successive additions of guest **14** to a solution of host **7** (2.9 mM).

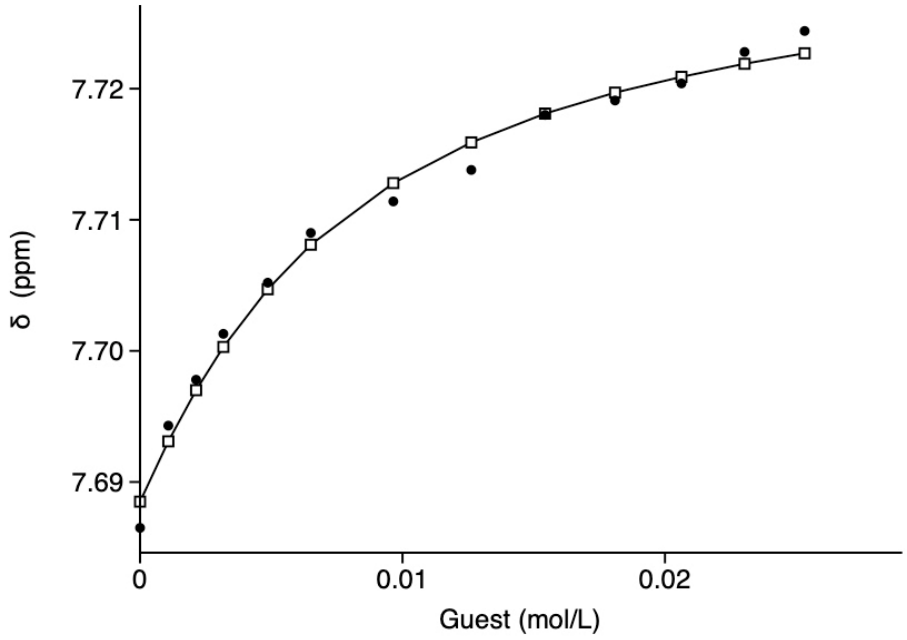

Fig. S16b. Chemical shifts of H_A (**7**, calculated: □, experimental: ●) as a function of guest concentration.

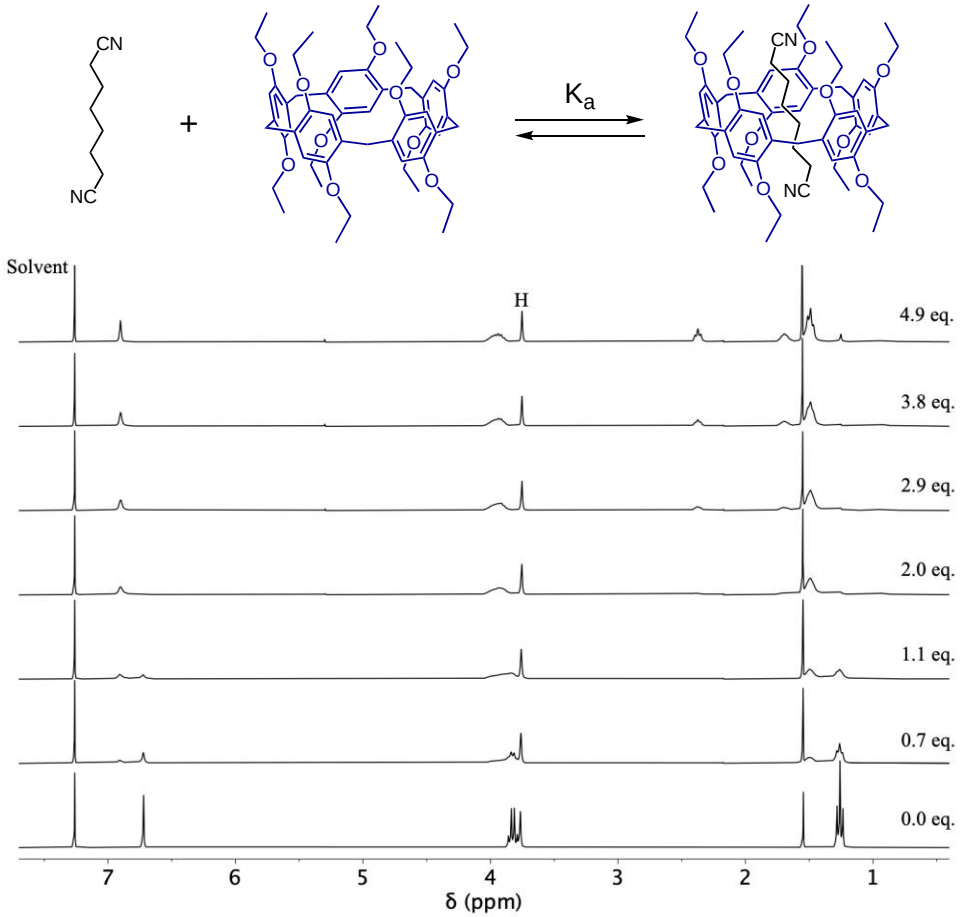

Figure S17a. Selected ^{1}H NMR spectra (300 MHz, $CDCl_3$, 298K) recorded upon successive additions of guest **9** to a solution of host **8** (2.1 mM).

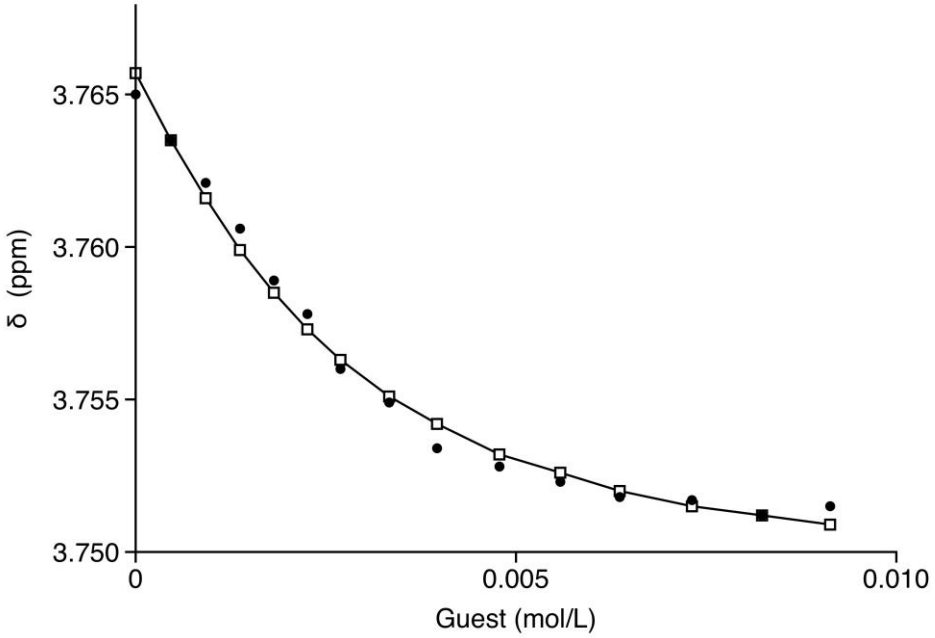

Fig. S17b. Chemical shifts of H_A (**8**, calculated: □, experimental: ●) as a function of guest concentration.

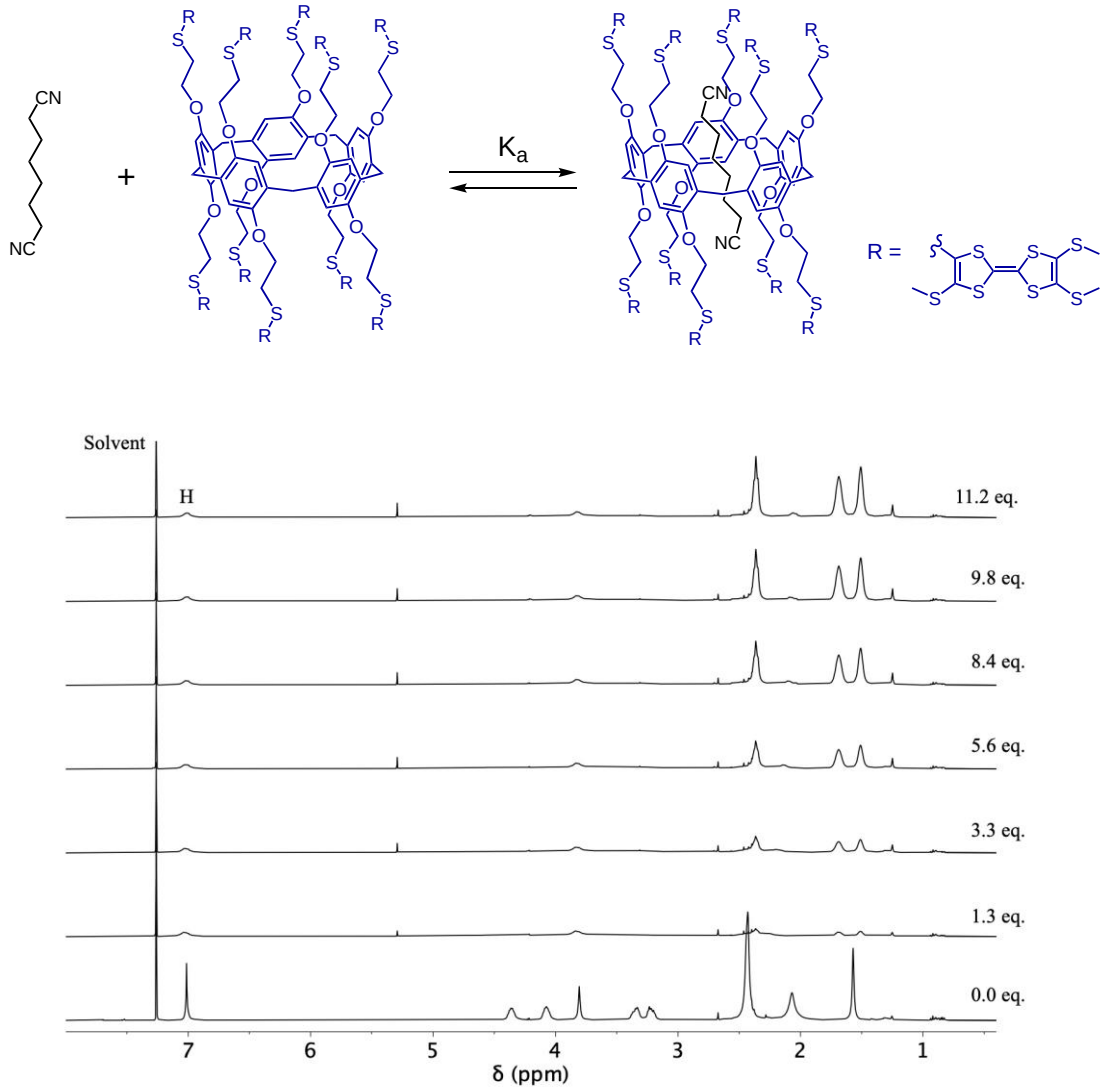

Figure S18a. Selected ^{1}H NMR spectra (400 MHz, $CDCl_3$, 298K) recorded upon successive additions of guest **9** to a solution of host **3b** (3.4 mM).

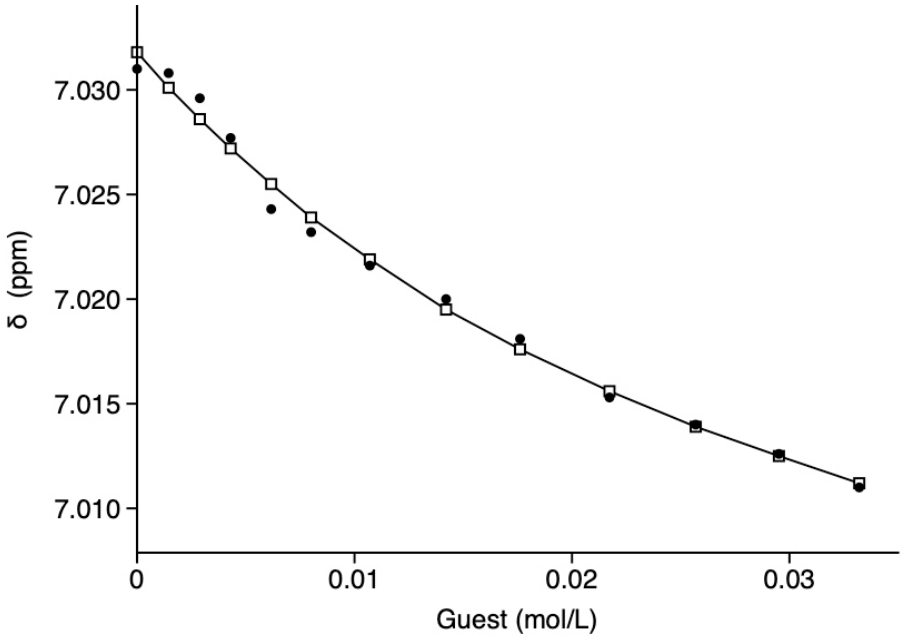

Fig. S18b. Chemical shifts of H_A (**3b**, calculated: □, experimental: ●) as a function of guest concentration.

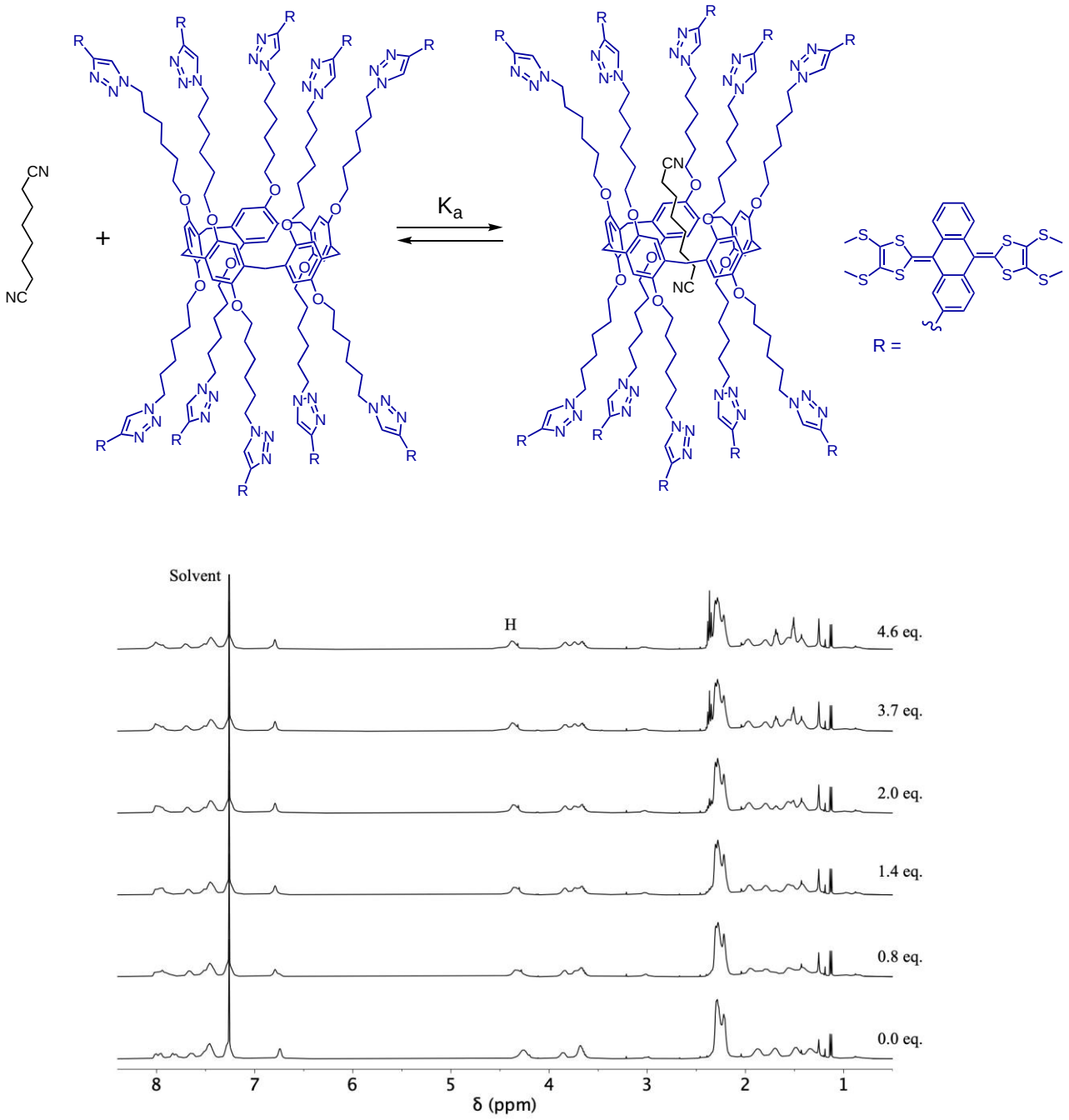

Figure S19a. Selected ^{1}H NMR spectra (400 MHz, $CDCl_3$, 298K) recorded upon successive additions of guest **9** to a solution of host **7** (2.2 mM).

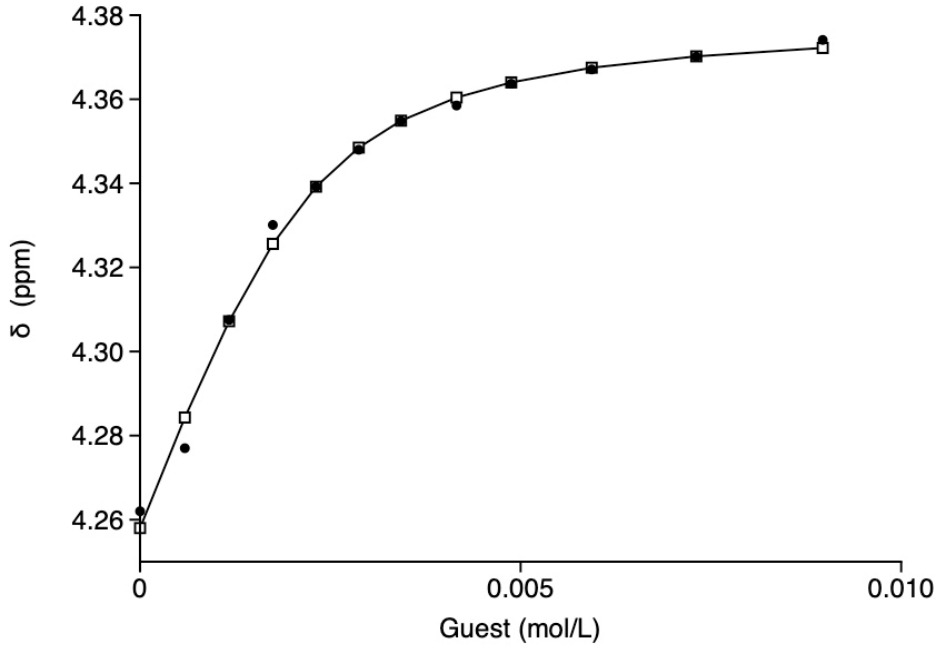

Fig. S19b. Chemical shifts of H_A (**7**, calculated: □, experimental: ●) as a function of guest concentration.

Calculated structures

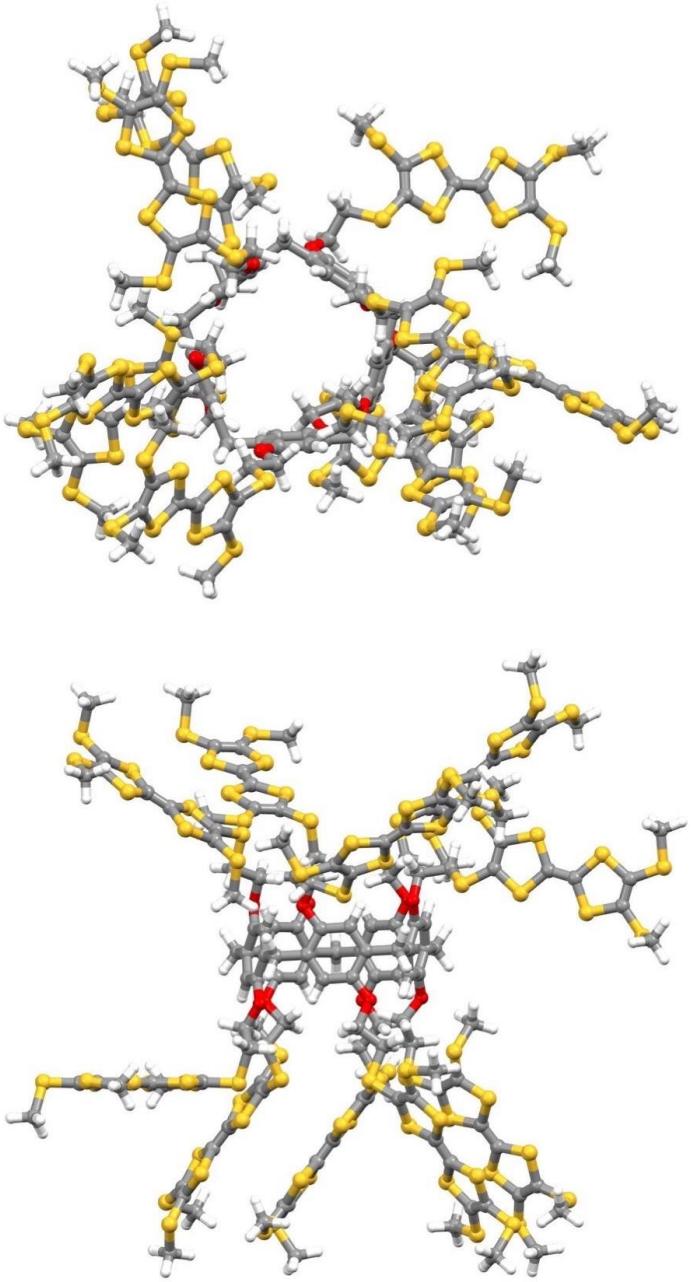

Fig. S20a. Front and top views of the calculated structure of compound **3b**.

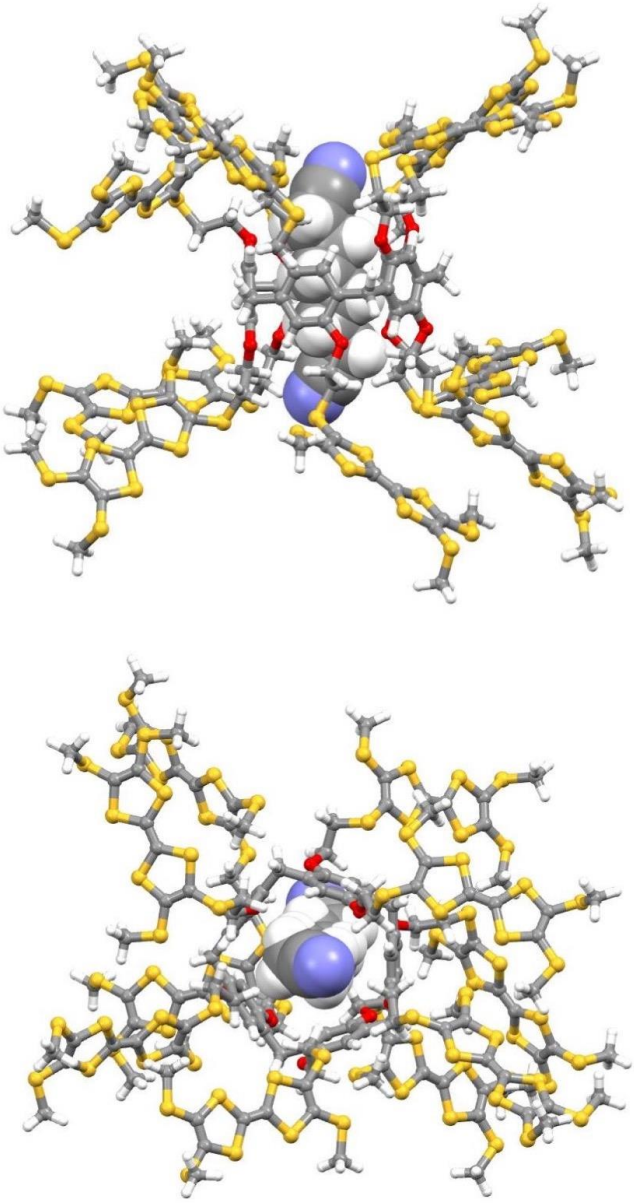

Fig. S20b. Front and top views of the calculated structure of inclusion complex **[9 ⊂ 3b]**.

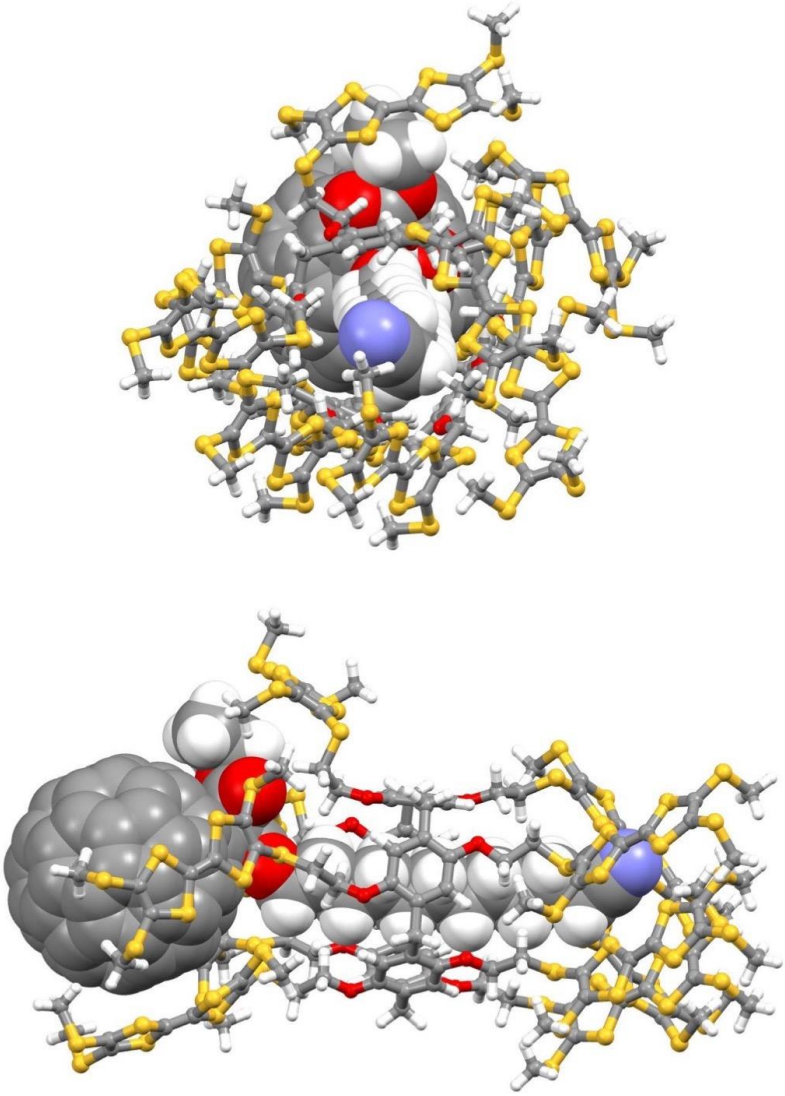

Fig. S20c. Top and front views of the calculated structure of inclusion complex **[14 ⊂ 3b]**.

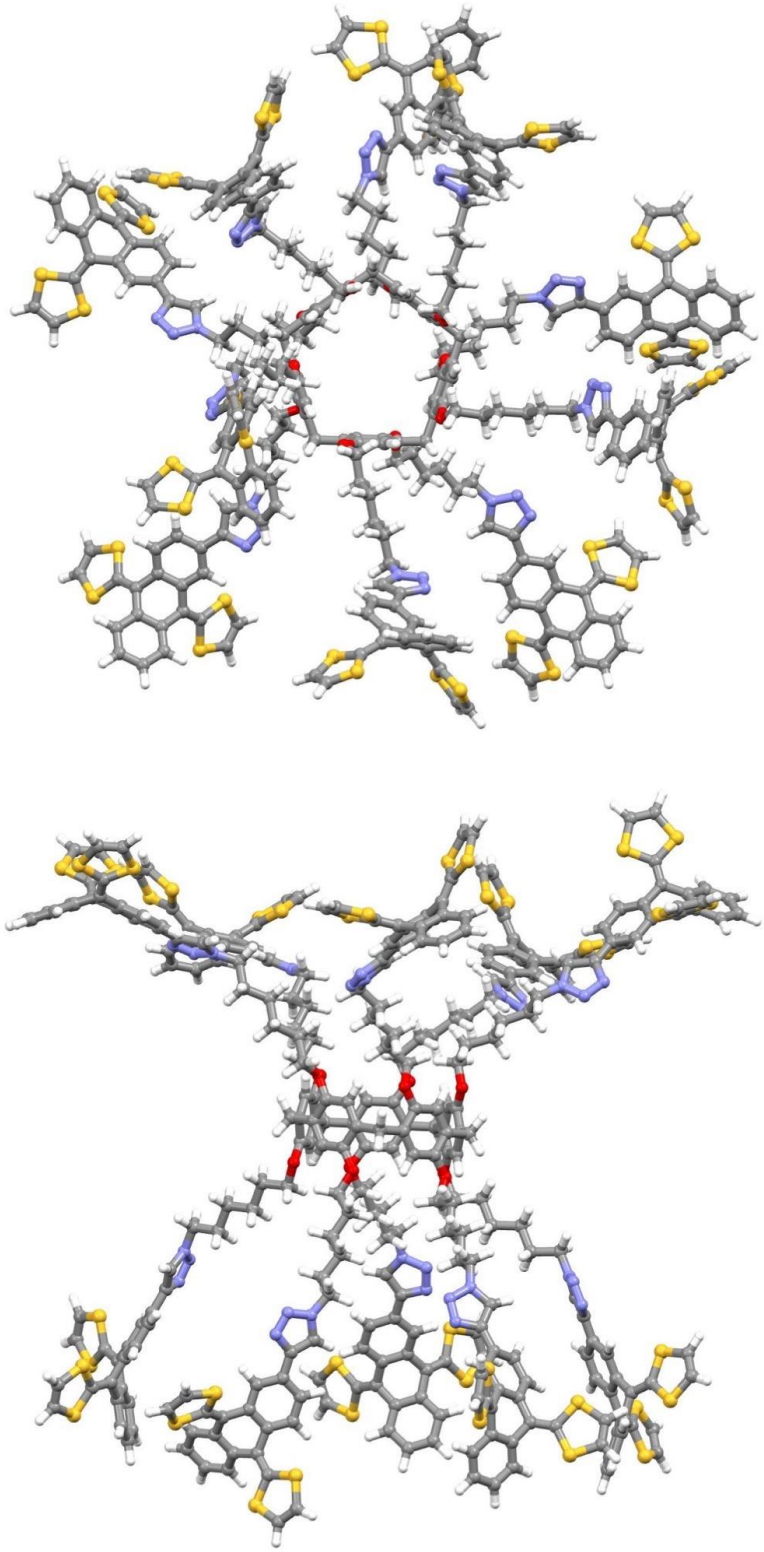

Fig. S20d. Top and front views of the calculated structure of compound **7**.

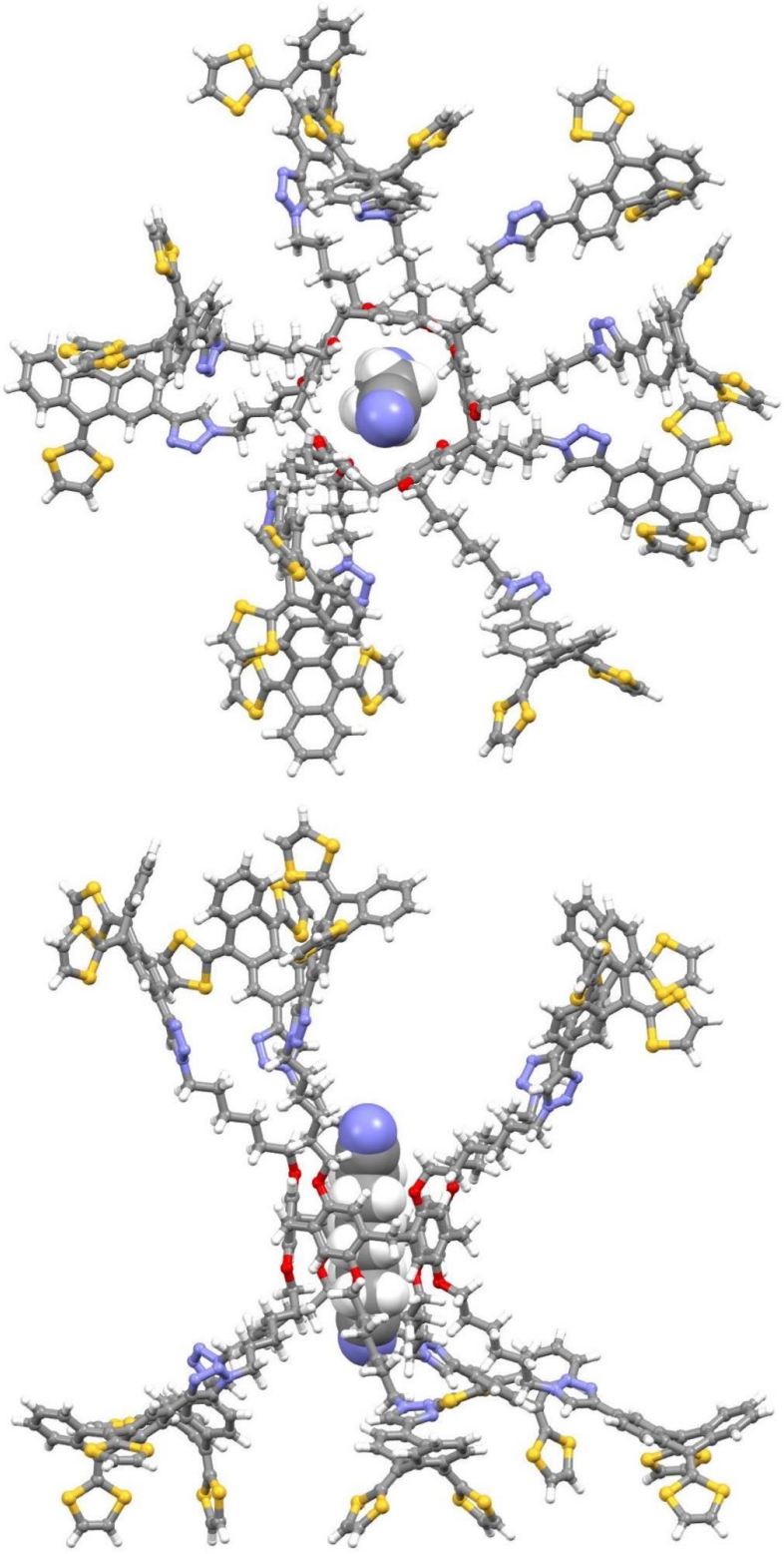

Fig. S20e. Top and front views of the calculated structure of inclusion complex **[9 ⊂ 7]**.

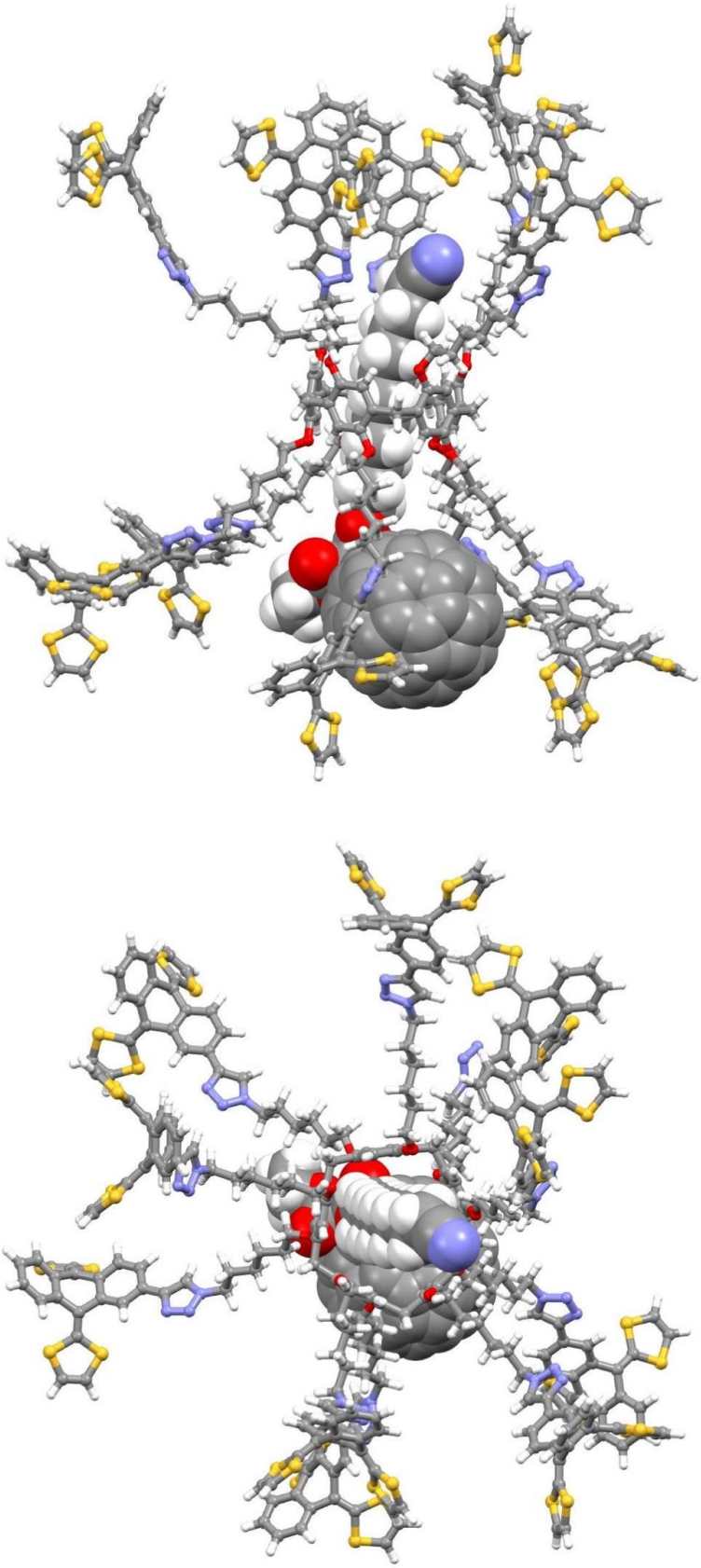

Fig. S20f. Front and top views of the calculated structure of inclusion complex **[14 ⊂ 7]**.